Determination of the Multipolarity of Nuclear Electromagnetic Transitions Using a Magnetic Pair Spectrometer*

E. K. WARBURTON, D. E. ALBURGER, A. GALLMANN,† P. WAGNER,† AND L. F. CHASE, JR.‡
Brookhaven National Laboratory, Upton, New York
(Received 2 August 1963)

An intermediate-image magnetic pair spectrometer has been modified so as to respond to positron-electron internal pairs emitted at large relative angles ($50° \lesssim \theta \lesssim 90°$) thereby making the pair-line transmission depend sensitively on the multipolarity of electromagnetic transitions above 2 MeV. The modification consists of a specially designed spiral baffle system which selects pairs emitted within 105° azimuthal sectors on opposite sides of the axis. Measurements are made of the net yield of an internal-pair-conversion coincidence line, both in the normal spectrometer operation (pairs with relative angles $0° \leq \theta \lesssim 90°$) and with the spiral baffle installed, giving a reduction ratio $R_\omega = Y_{\text{with baffle}}/Y_{\text{without baffle}}$. Experimental ratios were determined for 14 known transitions including $E0$, $E1$, $M1$, $E2$, $M2$, and $E3$ multipoles between 3 and 7 MeV. Theoretical calculations were carried out on the spectrometer transmission, when using the baffle, for $E0$, $E1$ through $E4$, and $M1$ through $M4$ transitions from nonaligned nuclei over a wide energy range. These transmissions were combined with previous calculations of the transmission without the baffle in order to derive curves of $R_\omega(l)$ versus transition energy for the various multipoles. A best fit to the experimental ratios for the known multipoles was made in the calculations by adjusting slightly the values of the mean spectrometer-entrance angle and the sector angle ω of the baffle. The various ratio curves thus obtained are spaced widely enough apart to allow clear multipole assignments to be made in most cases. For mixed transitions from aligned nuclei, calculations were made of correction factors to be applied to the experimentally determined ratios. It is shown how the correction factors can be derived from separate measurements of the angular distributions of the corresponding gamma rays. The method has been applied to a number of previously unassigned transitions in Be^{10}, B^{10}, C^{14}, and N^{14} leading to new spin and parity information on certain levels in these nuclei. In particular, it is found that the Be^{10} 6.18-MeV level and the C^{14} 6.58-MeV level are both 0^+ and the N^{14} 5.10-MeV level has odd parity.

I. INTRODUCTION

THE measurement of the correlation of the electron-positron pair in internal pair creation accompanying electromagnetic transitions of $\gtrsim 2$ MeV in light nuclei has proven[1–3] to be an effective method of determining the multipolarity of such transitions. The angular correlation is predicted to a high degree of accuracy by the Born approximation and is quite sensitive to the multipolarity of the transition.[4–8] One disadvantage of the method is that the low probability of internal pair creation relative to gamma-ray emission[5] makes it difficult to study low-yield reactions. Furthermore, in previous methods of studying pair correlations, the rather poor energy resolution of the electron and positron counters (Geiger counters[1] or plastic scintillators[2,3]) limited the investigations to rather simple spectra.

Recently, the efficiency of the Brookhaven magnetic lens intermediate-image pair spectrometer[9–11] has been calculated[12,13] as a function of transition energy for $E0$ and the first four orders (i.e., $l=1$ to 4) of El and Ml radiation. These calculations, which are based on the Born approximation results of Oppenheimer[4] and Rose,[5] point up the sensitivity of the spectrometer efficiency to the electron-positron angular correlation. Because of this sensitivity it was felt that the spectrometer could be modified to yield poor angular resolution but good energy resolution (1–3%) electron-positron angular correlation measurements which would amount to a determination of transition multipolarity. Tests making use of a specially designed charge-sensitive spiral baffle system soon convinced us that such was the case. This paper reports on theoretical efficiency calculations, the design of the baffle system, the measuring techniques employed, tests of the method for 14 known transitions including $E0$, $E1$, $M1$, $E2$, and $E3$ multipoles between 3 and 7 MeV, and results on the assignment of multipolarities to some transitions in Be^{10}, B^{10}, C^{14}, and N^{14}.

* Work performed under the auspices of the U. S. Atomic Energy Commission.

† Permanent address: Institut de Recherches Nucléaires, Strasbourg, France.

‡ Permanent address: Lockheed Missiles and Space Research Laboratory, Palo Alto, California.

[1] S. Devons, G. Goldring, and G. R. Lindsay, Proc. Phys. Soc. (London) **A67**, 134 (1954); S. Devons and G. Goldring, *ibid.* 413 (1954); G. Goldring, *ibid.* 930 (1954).

[2] S. Gorodetzky, P. Chevallier, R. Armbruster, A. Gallmann, and G. Sutter, Nucl. Phys. **7**, 672 (1958); S. Gorodetzky, F. Scheibling, P. Chevallier, P. Mennrath, and G. Sutter, Phys. Letters **1**, 24 (1962).

[3] S. Gorodetzky, P. Chevallier, R. Armbruster, G. Sutter, and A. Gallmann, Nucl. Phys. **8**, 412 (1958); S. Gorodetzky, P. Chevallier, R. Armbruster, and G. Sutter, Nucl. Phys. **12**, 349 (1959).

[4] J. R. Oppenheimer, Phys. Rev. **60**, 164 (1941).

[5] M. E. Rose, Phys. Rev. **76**, 678 (1949).

[6] G. Goldring, Proc. Phys. Soc. (London) **A66**, 341 (1953).

[7] E. H. S. Burhop, *The Auger Effect* (Cambridge University Press, Cambridge, England, 1952).

[8] S. Devons and L. J. B. Goldfarb, in *Handbuch der Physik*, edited by S. Flügge (Springer-Verlag, Berlin, 1957), Vol. 42, p. 362.

[9] D. E. Alburger, Rev. Sci. Instr. **27**, 991 (1956).

[10] D. E. Alburger, Phys. Rev. **111**, 1586 (1958).

[11] D. E. Alburger, Phys. Rev. **118**, 235 (1960).

[12] D. H. Wilkinson, D. E. Alburger, E. K. Warburton, and R. E. Pixley, Phys. Rev. **129**, 1643 (1963).

[13] E. K. Warburton, D. E. Alburger, and D. H. Wilkinson, Phys. Rev. **132**, 776 (1963).

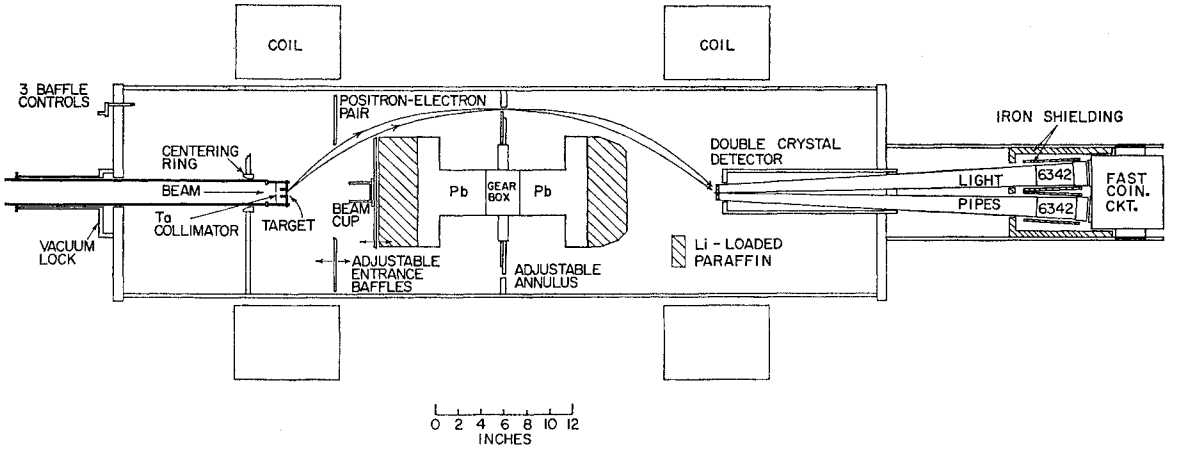

FIG. 1. Schematic diagram of the intermediate-image pair spectrometer.

II. EFFICIENCY CALCULATIONS

A. Pure Multiple Emission from Nonaligned Nuclei

Figure 1 is a schematic diagram of the intermediate-image pair spectrometer.[9–13] The beam direction defines an axis of cylindrical symmetry which we take to be the z axis (for definiteness we take a right-handed coordinate system with the x axis horizontal). The mean polar-angle α with which electrons or positrons must be emitted from the target in order to be focused through the annulus onto the detector is a constant of the spectrometer. If we designate the azimuthal angle (measured from the x axis) of the electron (or positron) at the moment of emission as $\phi_-(\phi_+)$, then ϕ_- varies from 0 to 2π, as does ϕ_+. We designate the azimuthal angle between an electron-positron pair at the moment of emission as $\phi=\phi_--\phi_+$, and adopt the convention that ϕ varies from $-\pi$ to π. The relationship between ϕ and the angle θ between the pair components at the moment of emission is[12]

$$\cos^2(\theta/2)=1-\sin^2\alpha\,\sin^2(\phi/2)\,, \qquad (1)$$

so that θ varies from 0 to 2α as ϕ varies from 0 to π.

Positron-electron pairs from the target are focused onto the detector if the energies of the components are the same (the effects of finite energy resolution are negligible[12]), i.e., $E_+=E_-=\frac{1}{2}(E_\gamma-1.022)$ MeV; or $W_+=W_-=\frac{1}{2}k$, where $W_\pm=E_\pm+1$, and k is the transition energy in units of m_0c^2.

We consider for the time being unmixed multipole radiation emitted from levels for which the magnetic substates are equally populated. The probability per unit energy interval, for the condition $W_+=W_-=\frac{1}{2}k$, that the β_+ and β_- particles are emitted with an azimuthal angle between them in the range ϕ to $\phi+d\phi$ is designated by $\gamma_l(\phi)$. The $\gamma_l(\phi)$ are obtained from the Born approximation results of Oppenheimer[4] and of Rose,[5] and are given implicitly by Wilkinson *et al.*[12] In Fig. 2 normalized plots of $\gamma_l(\phi)$, i.e., $\gamma_l(\phi)/\gamma_l(0)$, are shown for 6-MeV $E0$, $E1$, and $M1$ transitions for a polar-angle α equal to 45.7°.

In previous measurements[1–3] of electron-positron angular correlations the method used was to integrate over the β_+, β_- energy spectra. The resulting angular correlations are quite sensitive to multipolarity but not as much so as those obtained for $W_+=W_-=\frac{1}{2}k$ (Fig. 2). This is illustrated by comparing the ratio of the coincidence rates for θ equal to 0 and $\pi/2$ given by Rose[5] for the energy-integrated angular correlation to the same ratio which results from the constraint $W_+=W_-=\frac{1}{2}k$. For 6-MeV $E1$ and $M1$ transitions the former are[14] 14 and 28, respectively, while the latter ratios are 25 and 100, respectively.

Because of this extreme sensitivity of $\gamma_l(\phi)$ to multipolarity, it was felt that in many cases a "poor geometry," i.e., poor angular resolution, two-point correlation would suffice to distinguish the multipolarity of a transition. A "good geometry" determination of

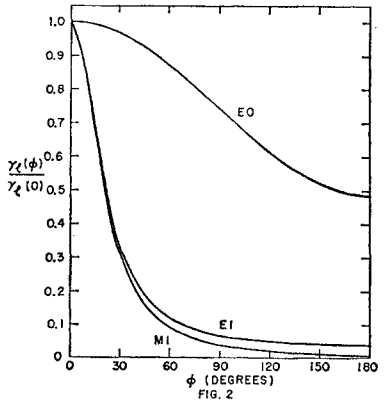

FIG. 2. Angular correlation of electron-positron pairs for 6-MeV $E0$, $E1$, and $M1$ transitions. The predicted relative coincidence rate for the intermediate-image spectrometer is shown as a function of the azimuthal angle ϕ between the pairs at the moment of emission.

[14] Taken from Figs. 1 and 2 of Ref. 5.

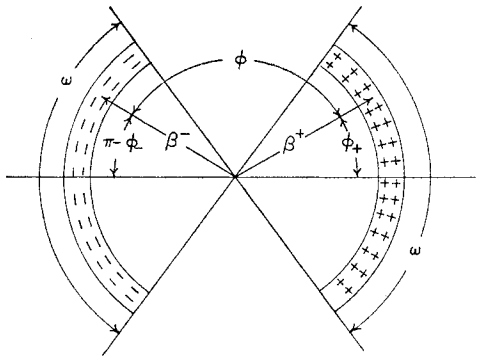

FIG. 3. Schematic polar diagram illustrating the emission sectors at the source defined by an idealized baffle system for the pair spectrometer. The baffle allows transmission only of positrons (β_+) for which $-\omega/2\leq\phi_+\leq+\omega/2$ and electrons (β_-) for which $\pi-\omega/2\leq\phi_-\leq\pi+\omega/2$, where $\phi_\pm$ are the azimuthal angles of the $\beta_\pm$ at the moment of emission.

the complete angular correlation function with the relatively low efficiency magnetic-lens spectrometer would take a prohibitive amount of time if the energy capabilities of the spectrometer are to be taken advantage of.

The scheme which was adopted is to compare the intensity of a given pair line obtained with a baffle inserted in the spectrometer such that only pairs with $\phi>\phi_{\min}$ are detected to the intensity of the same pair line obtained with the spectrometer operating under normal conditions. The value of $\phi_{\min}$ used will be a compromise between intensity and sensitivity to multipolarity. Since the pair-line intensity in the second instance is mostly due to pairs with a small angular separation between them, the ratio of these two intensities is essentially a "poor geometry" measure of the $\phi\gtrsim\phi_{\min}$ to $\phi\simeq 0$ coincidence rates. If $\phi_{\min}$ is sufficiently large this ratio will distinguish between various multipolarities.

In order to clarify the efficiency calculations we consider an idealized baffle which is a good approximation to the one actually used. As illustrated schematically in Fig. 3, this baffle stops all positrons except those for which ϕ_+ is between $+\frac{1}{2}\omega$ and $-\frac{1}{2}\omega$ and all electrons except those for which ϕ_- is between $\pi+\frac{1}{2}\omega$ and $\pi-\frac{1}{2}\omega$, where ω is the sector angle of the baffle. In this case $\phi_{\min}$ is $\pi-\omega$. The ratio of the coincidence rate (pair-line intensity) with baffle to that without baffle is given experimentally by

$$R_\omega'=(Y_{\text{with baffle}}/Y_{\text{without baffle}}), \tag{2}$$

where Y is the number of counts after background subtraction at the peak of a pair-coincidence line per transition, and is given theoretically by the ratio of spectrometer efficiencies with and without baffle,

$$R_\omega(l)=\mathcal{E}_l(\omega)/\mathcal{E}_l(2\pi), \tag{3}$$

where the calculation of $\mathcal{E}_l(2\pi)(\equiv\mathcal{E}_l)$ has been described previously.[12,15] We wish to calculate $\mathcal{E}_l(\omega)$, the efficiency of the spectrometer with baffle. Following previous results[12] we write

$$\mathcal{E}_l(\omega)=\frac{f_\omega(k)T^2R}{8\pi^2}\frac{(\frac{1}{4}k^2-1)}{\frac{1}{2}k}\times\int_{-\omega/2}^{+\omega/2}d\phi_+\left[\int_{\pi-\phi_+-\omega/2}^{\pi-\phi_++\omega/2}\gamma_l(\phi)d\phi\right]=4\pi f_\omega(k)T^2R\mathcal{E}_l'(\omega), \tag{4}$$

where k is the transition energy in units of m_0c^2, T is the transmission of the spectrometer (without baffle) for monoenergetic electrons expressed as a fraction of a sphere and R is the momentum resolution $\Delta p/p$ for the pair line. The factor $f_\omega(k)$ which corrects for counting rate losses in the baffle and detector system,[12] is, in principle, a function of both ω and k. The limits of integration follow from the geometry of Fig. 3. We define $C(\omega)\equiv f_\omega(k)/f_{2\pi}(k)$. As discussed in Sec. IVB, $C(\omega)$ is quite insensitive to k and ω and is assumed constant in the following discussion. Then,

$$R_\omega(l)=C(\omega)[\mathcal{E}_l'(\omega)/\mathcal{E}_l'(2\pi)]. \tag{5}$$

The $\mathcal{E}_l'(\omega)$ can be calculated in close analogy to the calculation of $\mathcal{E}_l'(2\pi)$ described previously.[12] The result is

$$\mathcal{E}_{El}'(\omega)=A(l)\sum_{n=0}^{l+1}G_n(l)I_n(\omega) \tag{6a}$$

for El radiation, and

$$\mathcal{E}_{Ml}'(\omega)=B(l)\sum_{n=0}^{l+1}H_n(l)I_n(\omega) \tag{6b}$$

for Ml radiation. The $A(l)$, $B(l)$, $G_n(l)$ and $H_n(l)$ are given by Wilkinson *et al.*[12]

The factors $I_n(\omega)$ contain all of the dependence on α and ω, i.e.,

$$I_n(\omega)=(1/2\pi)(\sin^{2n-4}\alpha)J_n(\omega), \tag{7}$$

where

$$J_n(\omega)=\frac{1}{2\pi}\int_{-\omega/2}^{+\omega/2}d\phi_+\left[\int_{\pi-\phi_+-\omega/2}^{\pi-\phi_++\omega/2}\frac{\sin^{2n}(\phi/2)d\phi}{[d^{-1}+\sin^2(\phi/2)]^2}\right] \tag{8}$$

[15] Throughout this paper R_ω' will be used to designate experimentally determined values of the ratio, R_ω will be used to designate values of the ratio for emission from nonaligned states. In general, the R_ω will be derived from the R_ω'. Only when the emitting state is known to be nonaligned will we have $R_\omega=R_\omega'=Y_{\text{with baffle}}/Y_{\text{without baffle}}$. So that no confusion arises, theoretically determined ratios will usually be designated by $R_\omega'(l)$ and $R_\omega(l)$ for pure multipole emission from aligned and nonaligned states respectively, and $R_\omega'(M,E)$ or $R_\omega(M,E)$ for a mixed Ml, $El+1$ transition.

with $d=(\frac{1}{4}k^2-1)\sin^2\alpha$. The integrals $J_n(\omega)$ are given by

$$J_0(\omega)=\frac{2}{\pi^2}J_0(2\pi)\int_0^{\tan(\omega/2)}\frac{\tan^{-1}aydy}{1+y^2}-\frac{d^2}{\pi(d+1)}\ln\left[\frac{1+d}{1+\frac{1}{2}d(1+\cos\omega)}\right], \quad (9a)$$

$$J_1(\omega)=\frac{2}{\pi^2}J_1(2\pi)\int_0^{\tan(\omega/2)}\frac{\tan^{-1}aydy}{1+y^2}+\frac{d}{\pi(1+d)}\ln\left[\frac{1+d}{1+\frac{1}{2}d(1+\cos\omega)}\right] \quad (9b)$$

and the recurrence formula for $n\geqslant 2$,

$$J_n(\omega)=\frac{1}{2\pi}\int_{-\omega/2}^{+\omega/2}d\phi_+\int_{\phi_+-\omega/2}^{\phi_++\omega/2}\cos^{2n-4}(\phi/2)d\phi-\frac{2}{d}J_{n-1}(\omega)-\frac{1}{d^2}J_{n-2}(\omega). \quad (9c)$$

The $J_n(2\pi)$ have been given previously,[12] and $a=(d+1)^{-1/2}$. The integral,

$$\int_0^{\tan(\omega/2)}\frac{\tan^{-1}aydy}{1+y^2},$$

was obtained numerically to better than 0.05% accuracy using an IBM-7090 computer.

For $E0$ transitions, we have

$$\mathcal{E}_{E0}'(\omega)=\frac{(\frac{1}{4}k^2-1)^3}{4\pi kI(E0)}\left[\frac{\omega^2}{4\pi^2}(1-\tfrac{1}{2}\sin^2\alpha)-\frac{\sin^2\alpha}{4\pi^2}(1-\cos\omega)\right], \quad (10)$$

where $I(E0)$ is an integral[12] which must be evaluated numerically. For $\omega=2\pi$, Eqs. (6) and (10) reduce to the appropriate formulas for $\mathcal{E}_l'(2\pi)$ given previously.[12]

In order to decide on the best baffle angle ω, the ratio $(4\pi^2/\omega^2)[\mathcal{E}_l'(\omega)/\mathcal{E}_l'(2\pi)]$ was calculated for El and Ml radiation with $l=1$, 2, 3, and 4 and for $E0$ radiation as a function of ω all for $k=12$ (6-MeV transitions). The results are shown in Fig. 4. By inserting the factor $4\pi^2/\omega^2$ the effect on $R_\omega(l)$ (Eq. 4) of the variation of solid angle with ω is taken out with the result that the variation of the sensitivity of $R_\omega(l)$ to multipolarity is seen more easily. From inspection of Fig. 4 we conclude that the best compromise between counting rate and sensitivity to multipolarity occurs in the range $90°\lesssim\omega\lesssim 120°$. In this range the difference between the various curves of Fig. 4 is on the average about 75% of that for $\omega=0°$ ($\omega=0°$ corresponds to $\phi_{\min}=\pi$).

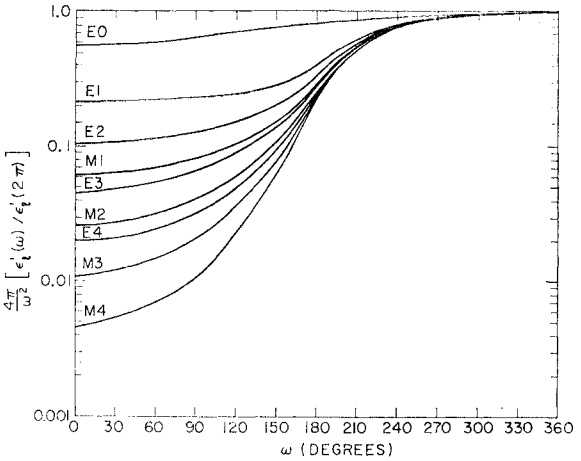

FIG. 4. The ratio of the reduced efficiency with a baffle of sector-angle ω to the reduced efficiency without the baffle per $\omega^2/2\pi$ as a function of the baffle sector angle ω for 6-MeV transitions.

B. Mixed Transitions from Aligned Nuclei

We now wish to generalize the efficiency calculations to include the effects of alignment, i.e., nonequal populations of the m_i substates of the emitting level, and the effects of interference between Ml and $El+1$ radiations. This has already been done[13] for the ordinary use of the spectrometer, i.e., $\omega=2\pi$ using the general expression for the emission of internal pairs from aligned nuclei.[16] The generalization to arbitrary ω is straightforward. For a Ml, $El+1$ mixture the efficiency is found by replacing $\mathcal{E}_l'(\omega)$, the efficiency for pure multipole emission and nonaligned nuclei (see Eq. 4), by

$$\eta_{M,E}'(\omega)=\frac{\eta_l'(\omega)+2x\eta_{l,l+1}'(\omega)+x^2\eta_{l+1}'(\omega)}{1+x^2}, \quad (11)$$

where x^2 is the ratio of the intensities of $El+1$ to Ml radiation for the associated gamma rays. The efficiency for pure Ml or $El+1$ radiation can be obtained from Eq. (11) by letting $x=0$ or ∞. In general, the spectrometer efficiency is related to that for pure multipole emission from nonaligned nuclei by,

$$\eta_{ll'}'(\omega)=\mathcal{E}_{l'}'(\omega)\sum_\nu A_\nu(ll')\Delta_\nu^{ll'}(\omega), \quad (12)$$

where $l'=l+1$ for the interference term, $l'=l$ for Ml or El radiation, and $\eta_{ll}'(\omega)\equiv\eta_l'(\omega)$.

The $\Delta_\nu^{ll'}(\omega)$ which are functions of α and k as well as of ω and l can be put in the form,

$$\Delta_\nu^{ll'}(\omega)=\sum_{n=0}^{l+1}H_n^{(\nu)}(ll')I_n(\omega)/\sum_{n=0}^{l+1}H_n^{(0)}(l)I_n(\omega), \quad (13a)$$

for Ml radiation ($l'=l$) or for the interference term in a

[16] E. K. Warburton (to be published).

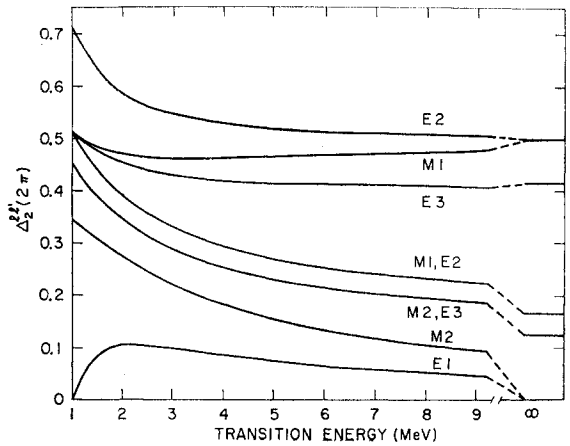

FIG. 5. The alignment factors $\Delta_2{}^{ll'}(2\pi)$ for $\alpha=45°$ versus transition energy from 1.022 to 9 MeV. The values for the high-energy limit are also shown.

mixed Ml, $El+1$ transition ($l'=l+1$). For El radiations,

$$\Delta_\nu{}^{ll}(\omega)=\sum_{n=0}^{l+1} G_n{}^{(\nu)}(l)I_n(\omega)/\sum_{n=0}^{l+1} G_n{}^{(0)}(l)I_n(\omega). \quad (13b)$$

The $H_n{}^{(\nu)}(ll')$ and $G_n{}^{(\nu)}(l)$ are functions of α and k. The $G_n{}^{(0)}(\equiv G_n)$ and $H_n{}^{(0)}(\equiv H_n)$ have been given previously.[12] We have calculated the $\Delta_\nu{}^{ll'}(\omega)$ for pure $E1$, $E2$, $M2$, and $E3$ transitions with $l_{\max}=4$ in the latter case, and mixed $M1$, $E2$ and $M2$, $E3$ transitions all for the two cases $\alpha=45°$, $\omega=2\pi$, and $\alpha=45°$, $\omega=120°$. The results for $\omega=2\pi$, which have been given previously,[13] are shown in Figs. (5) and (6) and the results for $\omega=120°$ are shown in Figs. (7) and (8). A value of 120° was used for ω since this value was found to give a good fit to the experimental results (see Sec. IVB); however, the $\Delta_\nu{}^{ll'}(\omega)$ are not too sensitive to ω and the general behavior of the $\Delta_\nu{}^{ll'}(120°)$ shown in Figs. (7) and (8) holds for ω in the approximate range 75–135°.

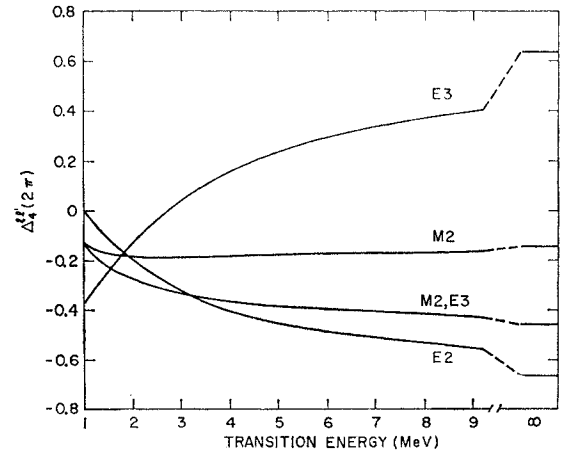

FIG. 6. The alignment factors $\Delta_4{}^{ll'}(2\pi)$ for $\alpha=45°$ versus transition energy from 1.022 to 9 MeV. The values for the high-energy limit are also shown.

The $A_\nu(ll')$ of Eq. 12 contain all the information on the alignment of the emitting level. They are related to the relative populations, $P(m_i)$, of the substates of the emitting level by

$$A_\nu(ll')=(-)^{l'-l}[(2l+1)(2l'+1)]^{1/2} \times C(ll'\nu;1,-1)\sum_{m_i m}(-)^{m+1}C(J_i l J_f;m_i m) \times C(J_i l' J_f;m_i m)C(ll'\nu;m,-m)P(m_i), \quad (14)$$

where J_i and J_f are the spins of the initial and final states of the transition, m_i and m_f are the projections of J_i and J_f on the z axis, $m=m_i-m_f$, $C(ll'\nu;1,-1)$ is a Clebsch-Gordan coefficient, and $\sum_{m_i}P(m_i)=1$.

The directional distribution of the competing gamma radiation is given by

$$W(\theta_\gamma)\sim\sum_\nu A_\nu P_\nu(\cos\theta_\gamma) \quad (15)$$

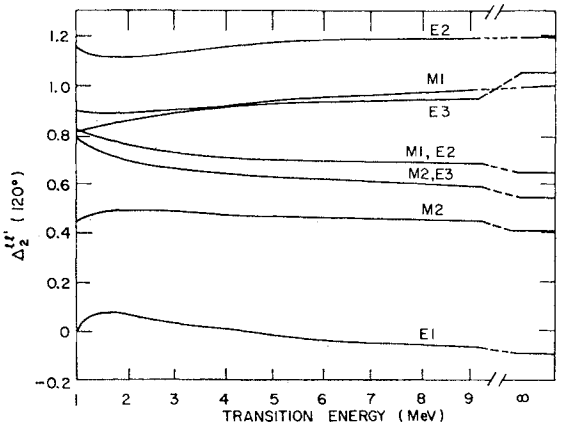

FIG. 7. The alignment factors $\Delta_2{}^{ll'}(120°)$ for $\alpha=45°$ versus transition energy from 1.022 to 9 MeV. The values for the high-energy limit are also shown.

where θ_γ is the polar angle of the direction of emission of the gamma radiation and

$$A_\nu=\frac{A_\nu(ll)+2xA_\nu(l,l+1)+x^2A_\nu(l+1,l+1)}{1+x^2}. \quad (16)$$

Thus, for pure multipole emission the $A_\nu(ll)$ of Eq. 12 can be determined from a measurement of the angular distribution of the competing gamma radiation.

The ratio of spectrometer efficiencies with and without baffle for a mixed Ml, $El+1$ transition from an aligned nucleus is

$$R_\omega'(M,E)=C(\omega)[\eta_{M,E}'(\omega)/\eta_{M,E}'(2\pi)]. \quad (17)$$

For pure multipoles the relation between $R_\omega'(l)$ and $R_\omega(l)$ (the efficiency ratio for nonaligned nuclei) is

$$R_\omega(l)=[\sum_\nu A_\nu(ll)\Delta_\nu{}^{ll}(2\pi)/\sum_\nu A_\nu(ll)\Delta_\nu{}^{ll}(\omega)]R_\omega'(l). \quad (18)$$

For pure multipoles the comparison between theory and experiment which is described later in this paper is most conveniently made by comparing experimentally obtained values of R_ω to the theoretical values of $R_\omega(l)$. The pair-spectrometer measurements actually yield values for R_ω'. However, Eq. (18) can be used to obtain values for R_ω from the measured R_ω'. This is illustrated in Secs. IV and V.

For pure $M1$ or $E1$ transitions $A_\nu(ll)=0$ for $\nu>2$ and for a given value of ω the ratio of Eq. (18) is a function of A_2 (11) only. This parameter which contains all the information on the degree of alignment is limited theoretically to the range $-1.0\leqslant A_2(11)\leqslant 0.5$. In Fig. 9 the variation of R_ω/R_ω' with $A_2(11)$ is shown for $\omega=120°$ and $\alpha=45°$. This figure illustrates that $E1$ transitions are quite insensitive to the degree of alignment but that $M1$ transitions are quite sensitive to the degree of alignment for large negative values of $A_2(11)$.

For mixed transitions the comparison between theory and experiment is most easily made by comparing R_ω' and $R_\omega'(M,E)$. The expression for $R_\omega'(M,E)$ is obtained from Eq. (17). For an Ml, El' mixture ($l'=l+1$) we have

$$R_\omega'(M,E)=\frac{R_\omega(l)+[\mathcal{E}_{l'}'(2\pi)/\mathcal{E}_l'(2\pi)]R_\omega(l')x^2+N_{ll'}(\omega)}{1+[\mathcal{E}_{l'}'(2\pi)/\mathcal{E}_l'(2\pi)]x^2+N_{ll'}(2\pi)}. \quad (19)$$

The term $N_{ll'}(\omega)$ takes account of alignment effects and is zero for nonaligned nuclei. For an $M1$, $E2$ mixture $N_{ll'}(\omega)$ is given by

$$N_{ll'}(\omega)=[\Delta_2{}^{ll}(\omega)A_2(ll)+2x\Delta_2{}^{ll'}(\omega)A_2(ll')]R_\omega(l)+[\Delta_2{}^{l'l'}(\omega)A_2(l'l')+\Delta_4{}^{l'l'}(\omega)A_4(l'l')]\times[\mathcal{E}_{l'}'(2\pi)/\mathcal{E}_l'(2\pi)]x^2R_\omega(l') \quad (20)$$

with $l=1$, $l'=2$.

III. DESIGN OF THE BAFFLE SYSTEM

There are two spectrometer constants which had to be determined more accurately than had been done previously[9] before the spectrometer could be used for the present application. These are the polar emission angle α and the angle β through which electrons and positrons turn between the target and the detector. An accurate measurement of α is desirable because $R_\omega(l)$ is quite sensitive to this angle, while the turning angle β must be known with fair accuracy in order to design the baffle system.

The angle α was determined by making transmission measurements with a small auxiliary baffle having an annular opening 1.5 mm wide and 1 in i.d. This was centered on the axis and could be moved axially on a screw just in front of the normal source position. With the spectrometer magnetic field set to focus the $K-1.06$-MeV internal conversion line from a Bi^{207} source, the auxiliary baffle was screwed in and out until the position of maximum detector yield was determined. A mean polar-emission angle of $45.7°\pm1.0°$ was obtained from the source-annulus geometry. Calculations showed that the correction for the bending of the orbit toward the axis is negligible for the distance of about 0.5 in. between the source and the small annulus.

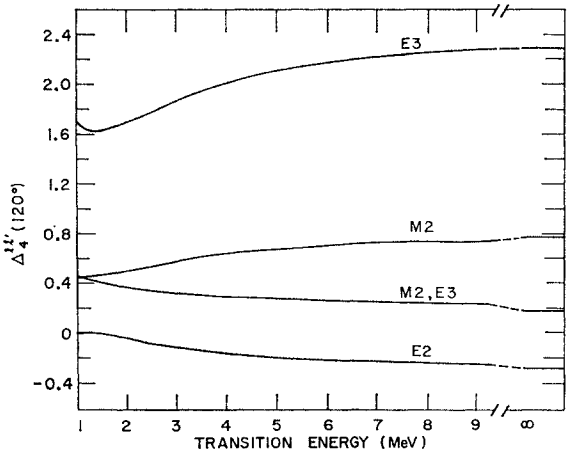

FIG. 8. The alignment factors $\Delta_4{}^{ll'}(120°)$ for $\alpha=45°$ versus transition energy from 1.022 to 9 MeV. The values for the high-energy limit are also shown.

In order to measure the turning angle β two auxiliary baffles were employed. One consisted of a disk having a narrow radial slot located just in front of the Bi^{207} source. The second baffle blocked off all of the 15-in. diam central annulus except for 1.5 in. along the circumference corresponding to an azimuthal angle of 11.5°. With the spectrometer set to focus the Bi^{207} internal conversion line, the slotted baffle in front of the source was rotated until a yield of focused electrons was obtained. The difference between the azimuthal angles of the two apertures was equal to half the total turning angle. This result was checked by reversing the magnetic-field direction and by finding the corresponding azimuthal angle of the slotted baffle which allowed electrons to reach the detector. From these tests the angle β was determined to be $225°\pm5°$.

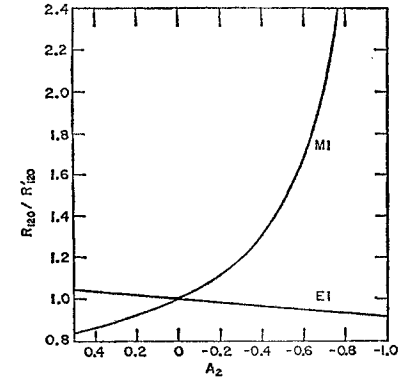

FIG. 9. The alignment correction R_{120}/R_{120}' for pure dipole radiation as a function of A_2 where the competing gamma-ray angular distribution is given by $W(\theta_\gamma)\sim1+A_2P_2(\theta_\gamma)$.

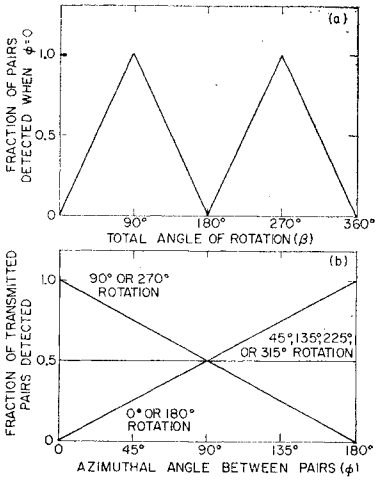

FIG. 10. Curve (a)—The average detection efficiency for positron-electron pairs with $\phi=0$ plotted versus the turning angle β of generalized axially-focusing spectrometers. Curve (b)—The average detection efficiency for pairs as a function of the angle ϕ (their separation in azimuthal angle) for the three special sets of Spectrometer angles β for which the efficiency when $\phi=0$ is 0, s.5, and 1.

Further studies of the turning angle β were made by using only the small slotted baffle in front of the source, the central annulus being unblocked. At the field setting for focusing the Bi^{207} line the yield in each of the semicircular detectors was measured as the slotted baffle was rotated. (In these tests as well as in all of the other work described in this paper the position of the detecting crystals was the same as described previously,[9,10] i.e., the front surfaces of the crystals were inside of the final focal point such that electrons were intercepted by the detector before they could reach the axis. Those electrons emitted at the mean entrance-angle α entered the crystals over an annular ring having half the radius of the crystals.) It was found that when the slotted baffle was rotated electrons were detected in each crystal over slightly less than 180° of variation in the azimuthal angle of the slotted baffle, while within each such sector the opposite crystal recorded no electrons. This established that there is a one-to-one correspondence between the azimuthal angle of emission from the source and the azimuthal angle of arrival of an electron at the detector, and that the turning angle β is relatively insensitive to the polar emission angle in the range $\alpha\pm\Delta\alpha$ where $\Delta\alpha=6°$ at the maximum spectrometer transmission setting. The turning angle $\beta=225°$ was confirmed by these tests.

The above tests suggested the need for a more detailed analysis of the normal operation of the pair spectrometer. In the initial development of the method of detection of positron-electron pairs by means of a thin-lens spectrometer Bame and Baggett[17] and Alburger[18] assumed that there was relatively little spatial correlation in the points of arrival of the two components at the detector and that the mode of detection of coincidences was one of so-called "statistical separation." Here the two components were assumed to arrive in opposite crystals 50% of the time, while in the remainder of cases the pairs enter the same crystal. However, our tests on the rotation of electrons in the intermediate-image spectrometer established that pairs do not enter the detector plane in a purely random fashion and that the mode of detection is not strictly "statistical." The actual detection efficiency not only might be different from 0.5 but it might depend on the angular correlation between the pair components.

We consider the general case of axial focusing of pairs onto two adjacent semicircular detecting crystals which are located in front of the final focal point. We require that a count be recorded only if the pairs enter opposite crystals and we neglect the effect of the absorber between the crystals. The turning angle β is taken as a variable. If we examine the particular case in which the β_+ and β_- components are emitted at 0° with respect to each other (i.e., $\phi=0$) we can calculate, by averaging over the azimuthal angle ϕ_- (or ϕ_+), the fraction of such pairs that is actually detected. Evidently for $\beta=0°$, 180°, 360°, etc., no pairs are detected since for any emission angle ϕ_- the two components always enter the detector at the same point and thus strike the same crystal. Similarly for $\beta=90°$, 270°, etc., the pairs always enter opposite crystals and they are all detected. In Fig. 10(a) the detection efficiency for pairs with $\phi=0$ is plotted versus the spectrometer turning angle β. It may be noted that for $\beta=45°$, 135°, 225°, and 315° the efficiency for detecting such pairs is 0.5.

Let us next consider what happens to the detection efficiency if we select certain values for the spectrometer constant β and allow ϕ to vary. Figure 10(b) illustrates three cases of special interest, corresponding to points in Fig. 10(a) where the efficiency for pairs with $\phi=0$ is 0, 0.5, and 1. Each curve of Fig. 10(b) was calculated by averaging over the complete range of ϕ_- for given values of β and ϕ. As shown in Fig. 10(b) we find that the detection efficiency for transmitted pairs depends on ϕ for any turning angle β not close to one of the values 45°, 135°, 225°, 315°, etc., and, hence, depends on the angular correlation between the β_+, β_-. However, for the above-mentioned set of turning angles the efficiency is exactly 0.5 independent of ϕ and thus independent of the angular correlation. Since by pure chance the β of our spectrometer is 225° the calculations discussed in the preceding section need not be modified to take into account a variation in the detection efficiency for transmitted pairs with the angular correlation between pairs.

In order to design a baffle which would impose the charge-acceptance conditions discussed in the last section, we first referred to some earlier work[19] in which a pair of spiral baffles had been constructed for investigat-

[17] S. J. Bame and L. M. Baggett, Phys. Rev. 84, 891 (1951).
[18] D. E. Alburger, Rev. Sci. Instr. 23, 671 (1952).
[19] D. E. Alburger, S. Ofer, and M. Goldhaber, Phys. Rev. 112, 1998 (1958).

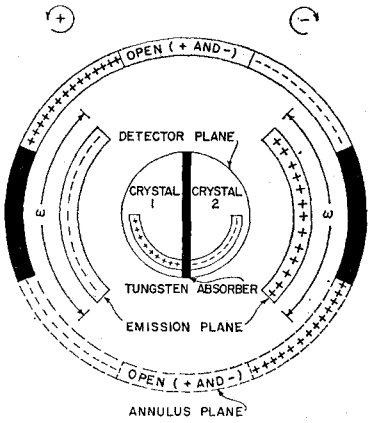

FIG. 11. Polar diagram (for our spectrometer having $\beta=225°$) illustrating the corresponding sectors for positrons and electrons leaving the source (emission plane), their passage through the spiral baffles in the upper half of the annulus plane, and their arrival in the detector plane. The spectrometer axis is perpendicular to the figure at the center of the diagram. A symmetrical baffle system in the lower half of the annulus plane accepts pairs from the emission plane having the opposite signs to those shown in the figure. The corresponding images for this case (not indicated) are in the upper half of crystal 2 for positrons and in the upper half of crystal 1 for electrons.

ing weak-positron emission from Eu^{152} in the presence of very strong beta-ray emission from this activity. Each of these baffles consisted of an array of 48 blades located adjacent to the annulus, one on either side. At these positions the angle of the blades with respect to the axis of the spectrometer resulting in maximum transmission for particles with the correct sign of charge had been found to be 18°. All blades of the baffles were, of course, tilted in the same sense. To selectively detect positrons or electrons merely required choosing the appropriate direction of current through the spectrometer coils. When only one set of baffles was used the spectrometer transmission for particles of the correct sign was 85% of the "no-baffle" transmission, but for particles of opposite sign (although at the same energy of about 1 MeV) only 1 in 10^5 reached the detector.

Evidently for the present application the direction of coil current must be fixed and the baffle must consist of an array of blades, some of which have a $+18°$ orientation allowing positrons to pass while others are oriented at $-18°$ to pass electrons. It was felt that a baffle system on only one side of the annulus (the detector side for convenience) would be sufficient for the present purposes. To explain how we arrived at the choice of baffle blade positions we refer to Fig. 11. The spectrometer axis is perpendicular to the page at the center of this polar diagram and the angular regions allowed for the projection of the trajectories of the β_+, β_- on three different planes are indicated, i.e., the projections on the planes of emission, annulus, and detector. We arbitrarily choose a clockwise rotation for negative electrons moving toward the detector. Let us follow a positive electron that is emitted in the horizontal plane on the right side of the axis, i.e., at $\phi_+=0°$. By the time such a positron arrives at the annulus it has turned to $\phi_+=112.5°$. At the end of its complete trajectory it has turned 225° and enters the detector at the angle $-135°$. Suppose we wish to transmit and detect positrons emitted within the 90° sector from $+45$ to $-45°$. The corresponding range of angles at the annulus is 157.5 to 67.5° and at the detector the range is -90 to 180°. Similarly, for negative electrons emitted on the opposite side of the axis and within the 90° sector $180°\pm45°$ these electrons turn clockwise, passing through the annulus in the angular range 22.5 to 112.5°, and they enter the detector in the angular range 0 to $-90°$.

Several interesting and useful features emerge from this analysis. First, we see that for the opposite 90° emission sectors the corresponding sectors at the annulus overlap, while at the detector the corresponding sectors are exactly in two adjacent quadrants. By orienting the semicircular crystal detectors as shown in Fig. 11 we expect to count all such positron-electron pairs. In the ordinary use of the spectrometer without the baffle it was shown earlier in this section that only half of all transmitted pairs are detected because of the 50% probability that the components enter opposite crystals. Thus, because of the fortunate circumstance that $\beta\cong225°$ for this spectrometer we have gained unexpectedly a factor of 2 in yield by the unit-detection efficiency when this type of particle selection is made.

As mentioned above, the positron and electron sectors at the annulus overlap. Since the selection of emission angles is completely determined by the spiral baffle at the annulus, it is evident that for the conditions described above the baffle should consist of electron and positron-transmitting blades on either side of a completely open space (with no blades) in the region where the sectors overlap as shown in the upper half of Fig. 11.

Under the conditions described above, i.e., β_+ emitted at $0°\pm45°$ and β_- emitted at $180°\pm45°$, the corresponding baffle system is completely contained above the horizontal plane passing through the axis. It occurred to us that a completely symmetrical set of baffles could be installed below the horizontal plane (rather than blanking off that region of the annulus) so as to detect those pairs where the β_- is emitted at $0°\pm45°$ and the β_+ is emitted at $180°\pm45°$, a situation just opposite to that described above. These baffles are indicated by the dashed lines in the lower part of Fig. 11. For this case the corresponding images (not indicated in Fig. 11) fall in the upper half of crystal number 1 for electrons and in the upper half of crystal number 2 for positrons. In taking advantage of this further factor of two greater yield than had been originally anticipated, one must be certain that by so doing, pairs emitted within the same sector are not recorded. That this is true may be seen by considering the case where both β_+ and β_- are emitted at 0°. The electron enters the detector plane at 135° after passing through the lower

half of the baffle, whereas the positron enters the detector plane at $-135°$ after passing through the upper half of the baffle. But because of the chosen orientation of the detectors both of these particles strike the same crystal and therefore do not register a coincidence. This holds true when both components are emitted anywhere in the same 90° sector. It is also true if the sector angles are made greater than 90°, provided that the sector angles are not allowed to be so large that in the detector plane the corresponding sectors "spill over" into the opposite crystals. One way to avoid the spill-over effect, and yet to make the sectors larger than 90°, is to displace the β_+ and β_- sectors at the annulus. The effect of doing this is that the mean angles of the emission sectors are no longer at exactly 180° with respect to each other.

In our final design we used a baffle system symmetrical in the upper and lower halves, similar to that indicated in Fig. 11 except that the angular openings of the overlapping β_+ and β_- sectors are each 105° and the relative mean angles between the β_+ and β_- sectors have been selected so as to prevent spill-over effects at the detector. The mean angle was 172°. The baffle blades were located so that their projections (at $+18°$ or $-18°$) on the annulus corresponded to the desired emission sector angles.

We may note here that, of the special spectrometer turning angles β (i.e., 45°, 135°, 225°, 315°, 405°, etc.) which have favorable properties for detecting pairs with no baffle or with a single spiral baffle system, not all of these angles are suitable for the *double* spiral baffle which we have described. It is only for every other pair of angles in this sequence, i.e., (135°,225°), (495°,585°) etc., that the defining sectors at the annulus for a given choice of positron-electron emission angles both lie completely on one side of a plane passing through the spectrometer axis, thereby allowing a symmetrical set of baffles to be constructed on the other side. While it may be possible to apply this general technique to an axially focusing spectrometer possessing a given turning angle β it would require a detailed analysis of each case in order to determine the utility of an instrument for this application. Thus, it might still be possible to construct a double spiral baffle system by placing the baffles at some intermediate location other than at the midplane. If the angular positions of the corresponding image sectors at the detector are not favorable it might be possible to place a larger detector well ahead of or well behind the focal point such that the images are intercepted when their relative angular orientations are more suitable. In the latter case the electrons could be allowed to cross the axis at the focus where an exit aperture could be installed.

In summary we have shown in this section that the detection of positron-electron pairs in the intermediate-image spectrometer does *not*, in fact, follow a strictly "statistical-separation" principle. However, the most fortunate fact that the rotation angle β in our spectrometer is 225° results in the following consequences; (a) in the ordinary use of the pair spectrometer without a spiral baffle the detection efficiency for transmitted pairs is 0.5 regardless of the angular correlation between the components, (b) with the baffle installed the detection efficiency for transmitted pairs is unity, and (c) it has been possible to design a baffle system giving four times the yield originally anticipated.

IV. TESTS OF THE TECHNIQUE

A. Experimental Procedure and Results

Our experimental procedure for determining values of R_ω' as defined by Eq. (2) was to record the pair-line spectrum of internal pair emission from a target under bombardment with a beam of fixed energy and intensity, first under normal operating conditions and then after installing the baffle described in the preceding section. Both measurements were made at the same spectrometer resolution setting and using the same bias conditions on the detector outputs. In order to install or remove the baffle, the vacuum had to be broken and the detector and end plate of the spectrometer had to be removed. (A new mechanical system has now been installed which allows the baffle to be moved in or out without breaking vacuum.) Particular care was taken to normalize the baffle-out and baffle-in spectra to the same number of target reactions. Three methods of normalization were used. The integrated beam current served as the reference if it was found that the intensities of given lines repeated indicating negligible effects of target deterioration or carbon buildup. This was true for most of the cases studied. However, in several cases, the yield did not remain proportional to the integrated beam current. In these cases the normalization was provided more reliably by monitoring the gamma rays from the target. A magnetically shielded 5-in.×5-in. NaI crystal detector located 8 ft from the target (see Ref. 12) was used for this purpose. Another normalization technique was to refer the pair-coincidence counting rate to the sum of the singles counting rates in the two-side crystals recorded at the spectrometer-field setting corresponding to the peak of the pair line. In general, the singles counting rate varies quite slowly with magnetic-field setting and it is usually proportional at a given field setting to the pair-line yield. When the background is high or when the reaction is strongly resonant, in such a way that the coincidence and singles rates do not have the same resonance structure, this method may not be satisfactory. From a number of tests made when using targets that were stable in yield the sum of the singles counting rates in the two crystals when the baffle was installed was found to be 0.63 times the rate when the baffle was removed. This ratio together with the inte-

TABLE I. Summary of transitions and experimental conditions used to establish calibration ratios R_ω' for various multipoles.

No.	Transition	Spin-Parity	Reaction	Beam energy (MeV)	Target	Reference
1	C^{13} 3.09 → 0	$\frac{1}{2}^+ \rightarrow \frac{1}{2}^-$	$C^{12}(d,p)C^{13}$	2.54	0.4 mg/cm², C^{12}	a
2	N^{14} 5.69 → 2.31	$1^- \rightarrow 0^+$	$C^{13}(d,n)N^{14}$	2.70	0.6 mg/cm², 66% C^{13}	b
3	Be^{10} 3.37 → 0	$2^+ \rightarrow 0^+$	$Be^9(d,p)Be^{10}$	2.0	3.7 mg/cm², Be^9	c
4	Li^6 3.56 → 0	$0^+ \rightarrow 1^+$	$Be^9(p,\alpha)Li^6$	2.83	3.7 mg/cm², Be^9	c
5	C^{13} 3.85 → 0	$\frac{5}{2}^+ \rightarrow \frac{1}{2}^-$	$C^{12}(d,p)C^{13}$	2.54	0.4 mg/cm², C^{12}	
6	C^{12} 4.43 → 0	$2^+ \rightarrow 0^+$	$Be^9(\alpha,n)C^{12}$	2.90	3.7 mg/cm², Be^9	d
7	N^{14} 4.91 → 0	$0^- \rightarrow 1^+$	$C^{13}(d,n)N^{14}$	2.70	0.6 mg/cm², 66% C^{13}	b
8	N^{14} 5.69 → 0	$1^- \rightarrow 1^+$	$C^{13}(d,n)N^{14}$	2.70	0.6 mg/cm², 66% C^{13}	b
9	Be^{10} 5.96 → 0	$1^- \rightarrow 0^+$	$Be^9(d,p)Be^{10}$	3.25	3.7 mg/cm², Be^9	c
10	O^{16} 6.06 → 0	$0^+ \rightarrow 0^+$	$F^{19}(p,\alpha)O^{16}$	2.83, 1.88	1 mg/cm² CaF_2 on 0.5 mil Ni	e
11	C^{14} 6.09 → 0	$1^- \rightarrow 0^+$	$C^{13}(d,p)C^{14}$	2.70	0.6 mg/cm², 66% C^{13}	b
12	O^{16} 6.13 → 0	$3^- \rightarrow 0^+$	$N^{15}(d,p)N^{16}(\beta_-)O^{16}$	2.50	~5 mg/cm² TiN^{15} on 0.05 mil Ni	f
13	O^{16} 6.92 → 0	$2^+ \rightarrow 0^+$	$F^{19}(p,\alpha)O^{16}$	2.83	1 mg/cm² CaF_2 on 0.5 mil Ni	e
14	O^{16} 7.12 → 0	$1^- \rightarrow 0^+$	$F^{19}(p,\alpha)O^{16}$	2.83	1 mg/cm² CaF_2 on 0.5 mil Ni	e

[a] See Ref. 12. [b] See Ref. 20. [c] See Ref. 13. [d] See Ref. 11. [e] See Ref. 9. [f] See Ref. 10.

grated singles counts could be used for normalizing the baffle-in and baffle-out spectra from less reliable targets.

The net normalized amplitudes at the peak of a given line were used to determine the ratio R_ω'. This required the determination of the background at the center of a line which was done by interpolating between background levels on either side of the line. In all of the examples studied, the background with the baffle in place was smaller than with the baffle out, but it was also larger in proportion to the net intensity of the pair-coincidence line. The contribution of random coincidences to the background was usually small. The origin of the real-coincidence background in the pair spectrum from the bombardment of Be^9 with 2.7-MeV deuterons was examined in detail with the spiral baffle removed. In spite of the prolific yield of neutrons from this reaction it was found that when the annulus was closed the yield in all parts of the spectrum decreased to almost nothing. This showed that background was not being produced by the interaction of neutrons near the detector but rather by pairs coming from the vicinity of the target. From studies of the background with various source-mounting arrangements it was concluded that the major contribution to the real coincidence background results from pairs that emerge from the target and then scatter from material near the target into the spectrometer solid angle. Such pairs might be expected to possess little angular correlation and, hence, would be relatively more effective in the baffle-in runs. The lowest background in this particular case was obtained by cementing a Be foil over a 1-cm diam opening in an aluminum target support. This background was lower by about a factor of 3 than that obtained[13] with the previous target support.

Measurements of the ratio R_ω' were made on 14 transitions of known multipolarity including one $E0$, seven $E1$'s, three $E2$'s, one $M1$, one $M2$, and one $E3$. The transitions observed and the conditions used to study them are summarized in Table I. In all of the work the diameter of the beam spot was 3 mm and, in most cases, the spectrometer was set for maximum transmission (annulus width 17 mm) under which conditions the pair-line resolution (full width at half maximum) is 2.8% for lines that have no Doppler broadening. Some of the lines were measured at an annulus setting of 9 mm (1.8% resolution) in order to better resolve them from neighboring lines or to see if the ratio R_ω' depends on the resolution setting.

Calibration lines Nos. 1 and 5 were studied by using a 0.4-mg/cm² thick self-supporting carbon foil bombarded at the 2.5-MeV resonance in the $C^{12}(d,p)C^{13}$ reaction. Lines 2, 7, 8, and 11 were measured in the deuteron bombardment of a 0.6-mg/cm² thick carbon foil enriched to 66% in C^{13}.[20] Both of these carbon targets withstood deuteron beam currents of 3 μA. Lines 3, 4, 6, and 9 were all studied with the same 3.7-mg/cm² thick Be foil target. This was bombarded with deuterons to produce lines 3 and 9 by the (d,p) reaction, with protons to produce line 4 by the (p,α) reaction and with alpha particles to produce line 6 by the (α,n) reaction. This target could withstand 3 μA of protons or deuterons with no sign of deterioration but not more than 1 μA of alpha particles at 3 MeV. The target for lines 10, 13, and 14 consisted of 1 mg/cm² of CaF_2 vacuum evaporated onto a 0.5-mil thick Ni foil which was mounted so that the beam passed through the backing before striking the CaF_2 deposit. These lines resulted from the $F^{19}(p,\alpha)O^{16}$ reaction, the beam energy being chosen so that the 6.92- and 7.12-MeV pair lines were approximately equal in amplitude without the baffle. This was the least reliable of any of the targets since even at a beam current of 0.5 μA there was a gradual decrease of yield indicating target deterioration.

[20] D. E. Alburger and E. K. Warburton, Phys. Rev. 132, 790 (1963).

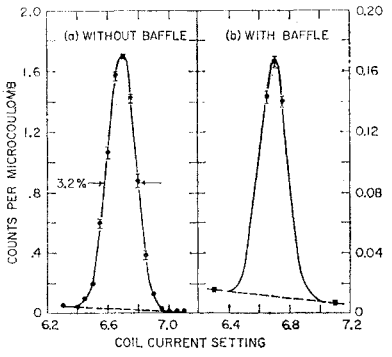

FIG. 12. The Li^6 3.56-MeV pair line obtained (a) without the baffle and (b) with the baffle.

In all of the cases cited thus far, the ratios R_ω' were measured on at least three separate occasions. Except for the lines occurring in the $F^{19}(p,\alpha)O^{16}$ reaction the ratios always repeated within the statistical errors. The ratios for lines 10, 13, and 14 have been assigned errors which are greater than statistical in order to allow for the poorer reproducibility of the various measurements.

A typical baffle-out baffle-in comparison is illustrated in Fig. 12. Curve (a) shows a complete run on the pair line from the Li^6 $3.56 \rightarrow 0$ transition occurring in the $Be^9(p,\alpha)Li^6$ reaction at $E_p = 2.83$ MeV (line No. 4 in Table I) without the baffle. Runs of this sort were made in order to locate accurately the position of the peak as well as its net intensity. With the baffle installed it was usually necessary to record only the peak point or a few points near the peak and also several background points on either side of the line in order to establish the interpolated background value at the peak position. This is illustrated in curve (b) of Fig. 12. The reliability of the spectrometer current regulator in reproducing peak positions (which were always the same with or without the baffle) justified this procedure and allowed better statistics to be obtained at the lower counting rates occurring with the baffle in place.

Line No. 12 was observed in the beta decay of N^{16} as formed by the $N^{15}(d,p)N^{16}$ reaction. The target consisted of TiN^{15} powder enriched to 95.6% N^{15} deposited from a water slurry onto a 0.05-mil thick Ni foil. The TiN^{15} deposit, estimated to be ~ 5 mg/cm^2 in thickness, was placed in the spectrometer such that the beam went through the Ni backing before striking the TiN^{15} target. A beam chopper and delayed electronic gating system[21] was used to make the N^{16} activity and to count the pair line of the 6.13-MeV transition during the beam-off portion of the cycle. In this experiment the resolving time of the coincidence circuit was reduced to 1 mμsec in order to cut down the random coincidence rate caused by the high intensity of the N^{16} beta rays. It was found convenient to check both the spectrometer momentum calibration and the operation of the fast coincidence circuit by turning off the chopper and observing the prompt 6.06-MeV $E0$ pair line occurring in the $N^{15}(d,n)O^{16}$ reaction. Measurements of the ratio R_ω' for the 6.13-MeV $E3$ line were made in the usual manner. For this line the background levels were higher than for any of the others studied and the statistical error assigned to R_ω' was, therefore, comparatively large. Furthermore, in the interpretation of the measured ratio allowance had to be made for the possible admixture of an unresolved 6.06-MeV $E0$ pair line which might be present due to a weak beta-ray branch of N^{16} to the O^{16} 6.06-MeV state. In previous work[10] it was found, in the normal spectrometer operation without a baffle, that the 6.06-MeV pair line in N^{16} decay was $\leqslant 10\%$ as strong as the 6.13-MeV $E3$ pair line and from this result it was deduced that the $\log ft$ value of the beta-ray transition to the 6.06-MeV 0+ first-excited state of O^{16} is $\geqslant 8.2$. As will be shown later, the ratio R_ω' for a 6-MeV $E0$ transition is about 5 times larger than for an $E3$ transition of this energy. Hence, with the baffle installed the relative intensity of the pair line of a possible 6.06-MeV $E0$ transition in the decay of N^{16} could be as much as 50% as strong as the pair line of the 6.13-MeV transition. At first it was hoped that a more sensitive search for the 6.06-MeV pair line in N^{16} decay could be made by using the baffle because of the factor of 5 enhancement of the relative intensity of this line. Although this experiment is sound in principle and may still be possible, it was felt from considerations of the statistics of the net yield and background at various spectrometer resolution settings that it would be difficult to improve appreciably on the previous result by using the baffle. At the 2.8% resolution used for measuring R_ω' for the 6.13-MeV pair line, the contribution to its peak intensity in the baffle-in measurement, resulting from a possible 6.06-MeV $E0$ line, would be about half of the peak intensity of the 6.06-MeV line and, thus, from the 50% limit mentioned above, the 6.13-MeV pair line could, at its peak, consist of as much as 25% of an $E0$ component. The error assigned on the low side of R_ω' for the 6.13-MeV line is, therefore, larger than on the high side.

All of the calibration lines except for Nos. 13 and 14 were measured at the maximum transmission setting (17 mm annulus width). Lines 3, 5, 9, 10, and 11 were also measured at 9 mm annulus width (1.8% resolution). Line No. 10 was the only one also measured at an annulus width of 6 mm (1.3% resolution). In none of these cases was there a dependence of the ratio R_ω' on the resolution setting that was apparent outside of the statistical errors. Values of R_ω' are given in Table II and they represent the weighted averages of all measurements at the two principal resolution settings used. We assume that all 14 transitions are pure, unmixed transitions having the multipolarities listed in Table II. With this assumption the alignment correction for obtaining R_ω from R_ω' is straightforward if the $A_\nu(ll)$ values of Eq. (18) are known. The values of R_ω given in the last column of Table II were obtained using Eq. (18), the

[21] D. H. Wilkinson, D. E. Alburger, A. Gallmann, and P. F. Donovan, Phys. Rev. **130**, 1953 (1963).

TABLE II. Summary of the experimental ratios R_ω' for the calibration lines, the angular-distribution correction factors and the corrected ratios R_ω.

No.	Transition	Multipolarity	R_ω'	A_ν	R_ω
1	C^{13} 3.09 → 0	$E1$	0.185±0.008	$A_2=0$	0.185±0.008
2	N^{14} 5.69 → 2.31	$E1$	0.168±0.012	$A_2=0.0\pm0.1$	0.168±0.012
3	Be^{10} 3.37 → 0	$E2$	0.133±0.005	$A_2=+(0.03\pm0.05)$ $A_4=+(0.06\pm0.05)$	0.130±0.006
4	Li^6 3.56 → 0	$M1$	0.092±0.002	$A_2=0$	0.092±0.002
5	C^{13} 3.85 → 0	$M2$	0.057±0.004	$A_2=+(0.42\pm0.04)$ $A_4=-(0.1\pm0.1)$	0.056±0.005
6	C^{12} 4.43 → 0	$E2$	0.100±0.005	$A_2=+(0.09\pm0.02)$ $A_4=-(0.08\pm0.03)$	0.097±0.005
7	N^{14} 4.91 → 0	$E1$	0.112±0.010	$A_2=0$	0.112±0.010
8	N^{14} 5.69 → 0	$E1$	0.119±0.010	$A_2=0.0\pm0.1$	0.119±0.010
9	Be^{10} 5.96 → 0	$E1$	0.102±0.003	$A_2=0.0\pm0.1$	0.102±0.003
10	O^{16} 6.06 → 0	$E0$	0.265±0.005	$A_2=0$	0.265±0.005
11	C^{14} 6.09 → 0	$E1$	0.105±0.003	$A_2=0.0\pm0.1$	0.105±0.003
12	O^{16} 6.13 → 0	$E3$	$0.055^{+0.008}_{-0.013}$	$A_2=A_4=0$	$0.055^{+0.008}_{-0.013}$
13	O^{16} 6.92 → 0	$E2$	0.065±0.005	...	0.065±0.005
14	O^{16} 7.12 → 0	$E1$	0.090±0.010	$A_2=0.0\pm0.3$	0.090±0.010

$A_\nu(ll)$ listed in the fifth column of Table II, and the $\Delta_\nu{}^{ll}(2\pi)$ and $\Delta_\nu{}^{ll}(120°)$ of Figs. 5–8. A few words of explanation are necessary as to the origin of the $A_\nu(ll)$'s given in Table II.

For lines 1, 4, 7, and 10 the transitions are from an initial state with $J_i=0$ or $\frac{1}{2}$; thus, there can be no preferred direction in space for these transitions and the alignment correction is zero, i.e., $A_\nu=0$ for $\nu>0$. The O^{16} 6.13 → 0 transition (No. 12) was initiated by the β decay of N^{16} and thus the alignment correction for this transition is also rigorously zero. For lines 2, 8, 9, and 11 the initial state is formed by the (d,p) or (d,n) reaction which proceeds predominantly by a stripping mechanism with the capture of $l=0$ neutrons or protons. For this reaction mechanism the initial state is formed unaligned so that the A_2 coefficient of these transitions, all of which are $E1$, were assumed to be 0.0 ± 0.1. The assumed uncertainty is our arbitrary estimate of the possible deviations from isotropy due to departure from a pure stripping reaction mechanism. The O^{16} 6.72 → 0 and 7.12 → 0 transitions (Nos. 13 and 14) were observed using a fairly thick F^{19} target (Table I) and thus the A_2 and A_4 coefficients for these transitions are averages over the values for many resonances in the compound nucleus and are probably small. For the O^{16} 7.12 → 0 transition $A_\nu=0$ for $\nu>2$ since the transition is $E1$, and we arbitrarily assume $A_2=0.0\pm0.3$. The $E2$ O^{16} 6.72 → 0 transition can have both A_4 and A_2 different from zero and since the alignment correction depends on the relative values of these coefficients it is difficult to give a meaningful estimate without some knowledge of the A_ν's. For this transition we assume $R_\omega=R_\omega'$ and give the experimental uncertainty in R_ω only.

The A_ν coefficients for the Be^{10} 3.37 → 0 (No. 3) and C^{12} 4.43 → 0 (No. 6) transitions were obtained from measurements of the angular distributions of the accompanying gamma radiation. The results for the angular distribution of the Be^{10} 3.37 → 0 gamma transition have been reported previously.[13] For the C^{12} 4.43 → 0 transition we used the same target and bombarding conditions as were used to obtain the pair spectrometer results and the angular distribution was taken in the same manner as the previously described results for the Be^{10} 3.37 → 0 transition.

The only remaining transition to be discussed is the C^{13} 3.85 → 0 transition. If this transition is pure $M2$ the plane-wave stripping theory predicts[22]

$$A_2=0.5714Q_2,\quad A_4=-0.5714Q_4,$$

where Q_2 and Q_4 are attenuation coefficients, $0\leqslant Q_\nu\leqslant 1$, which are to be evaluated. The angular distribution of the $C^{12}(d,p)C^{13}$ (3.85 → 3.68) transition has been measured for deuteron energies between 1.6 and 3.2 MeV.[23] From these results we obtain $Q_2=0.74\pm0.06$ for E_d between 2.55 and 2.45 MeV. This gives $A_2=+0.42\pm0.03$, which is a model-independent result depending only on the assumption that the C^{13} 3.85 → 0 and 3.85 → 3.68 transitions are pure $M2$ and $E1$ transitions, respectively. The attenuation coefficient Q_4 can be evaluated using plane-wave stripping theory. The prediction is that $Q_4=0.34$ at $E_d=2.5$ MeV. However, any distortion effects are apt to decrease Q_4, and guided by results for the similar $C^{14}(d,p)C^{15}$ (0.75 → 0) transition[24] we take $Q_4=0.17\pm0.17$ which gives $A_4=-(0.1\pm0.1)$. We note that experiments[25] on the $C^{12}(d,p\gamma)C^{13}$ correlation proceeding through the C^{13} 3.85-MeV level at

[22] E. K. Warburton and L. F. Chase, Jr., Phys. Rev. **120**, 2095 (1960).

[23] L. F. Chase, Jr., R. G. Johnson, and E. K. Warburton, Phys. Rev. **120**, 2103 (1960).

[24] L. F. Chase, Jr., R. G. Johnson, F. J. Vaughn, and E. K. Warburton, Phys. Rev. **127**, 859 (1962).

[25] N. R. Fletcher, D. R. Tilley, and R. M. Williamson, Nucl. Phys. **38**, 18 (1962); T. S. Katman, D. R. Tilley, R. M. Williamson, D. G. Gerbe, J. M. Lacambra, and J. R. Sawers, Bull. Am. Phys. Soc. **8**, 11 (1963).

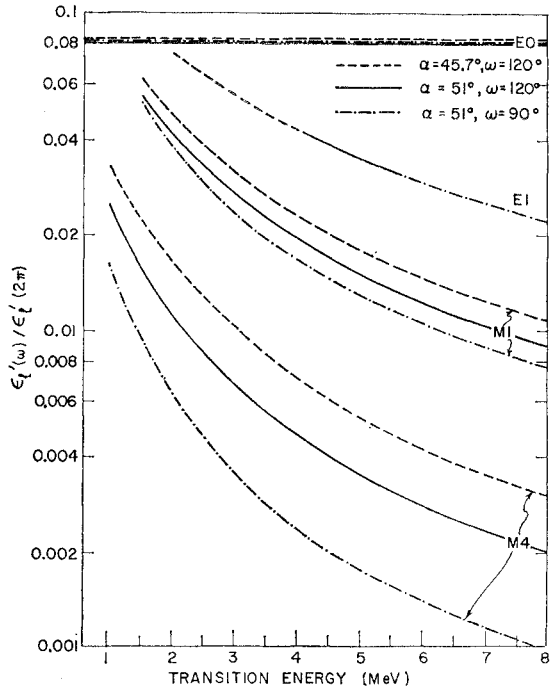

FIG. 13. Comparison of the ratio of reduced efficiencies with and without the baffle for $E0$, $E1$, $M1$, and $M4$ transitions for three sets of values of the angles α and ω. The three different $E1$ curves—which have been normalized at a transition energy of 6 MeV—are indistinguishable.

deuteron energies near 2.5 MeV are in fair agreement with plane-wave stripping theory but indicate some attenuation due to distortion effects thus giving added confidence in our estimate of A_4.

B. Comparison with Theory

The direct method of comparing the experimental results of Table II, i.e., the R_ω, to theory is to obtain the best values of ω and $C(\omega)$ from geometrical considerations and then to calculate the theoretical $R_\omega(l)$ from Eq. (5). In doing this we must make corrections for the deviation of the actual baffle system from the idealized one described in Sec. II. As described in Sec. III the actual baffle system has $\omega=105°$, but the azimuthal angle between the mean angle of positron emission and the mean angle of electron emission is 172° rather than 180° as assumed in the calculations of Sec. II. It turns out that this difference changes the $\mathcal{E}_l'(\omega)$ very little and if we use $[\mathcal{E}_l'(95°)+\mathcal{E}_l'(115°)]/2$ instead of $\mathcal{E}_l'(105°)$ the effect of this difference is taken account of to $\leqslant 3\%$ for $l\leqslant 2$. The other differences between the idealized baffle system and the actual one can all be absorbed into the $C(\omega)$ of Eq. (5). These differences arise from a loss in counting rate due to one member of the positron-electron pair striking either the baffle-blades or the tungsten absorber between the crystals. If both these losses were zero then $C(\omega)$ would be 4.0, independent of ω. The factor of four is due to the way $\mathcal{E}_l'(\omega)/\mathcal{E}_l'(2\pi)$ is calculated as explained at the end of Sec. III. The loss of transmission due to the baffle blades is estimated to cause a 10% reduction in the number of detected pairs. The loss of detected pairs in the tungsten absorber is estimated to be about 25% without the baffle and 0–15% with the baffle. The uncertainty in the latter case is due to inexact knowledge of the turning angle β and other details of the electron trajectories. Combining these factors we get $C(\omega)\cong 4.1$–4.8 for the geometry used. We note that $C(\omega)$ can have some dependence on k and l since the losses mentioned depend, in principle, on the angular correlation between the pairs. However, a study of the $\mathcal{E}_l'(\omega)$ and the spectrometer geometry showed that this dependence is quite small and can be simulated by a small change in ω.

Because $C(\omega)$ could not be obtained easily to better than about 20% from geometrical considerations the procedure actually used was to calculate the efficiency ratio $[\mathcal{E}_l'(\omega)/\mathcal{E}_l'(2\pi)]$ and to determine $C(\omega)$ from a comparison of this ratio and the experimental values of R_ω for the seven $E1$ transitions of Table II. The $E1$ transitions are well-suited for this purpose since they span a large range of transition energies and are quite insensitive to alignment effects (see Fig. 9). Initially $[\mathcal{E}_l'(\omega)/\mathcal{E}_l'(2\pi)]$ was calculated for $\omega=105°$ and for $\mathcal{E}_l'(\omega)=[\mathcal{E}_l'(95°)+\mathcal{E}_l'(115°)]/2$, both for $\alpha=45.7°$. A least-squares fit to the R_ω for the seven $E1$ transitions of Table II gave $C(\omega)=4.9$ and 4.7, respectively, for these two cases. This result indicates that the upper limit to the value of $C(\omega)$ calculated from the geometry is suitable. This corresponds to no loss of detected pairs in the tungsten absorber with the baffle in place.

When $R_\omega(l)$ was calculated for other multipolarities it was obvious that for $\omega=105°$ and $\alpha=45.7°$ the $R_\omega(l)$ were more sensitive to multipolarity than the experimental values of Table II. This indicates either that α is too large or ω too small. At this point it was decided to treat α, ω, and $C(\omega)$ as variable parameters and search for the best agreement with the experimental R_ω. The effect of decreasing α can be simulated to a good approximation by increasing ω. This is illustrated in Fig. 13, which shows relative theoretical values of $\mathcal{E}_l'(\omega)/\mathcal{E}_l(2\pi)$ for three different sets of values of α and ω for $E0$, $E1$, $M1$, and $M4$ transitions. The three sets are normalized so that the curves for $E1$ transitions coincide at 6 MeV. The important conclusion to be drawn from this figure is that the three curves for a given multipolarity are proportional to each other to a good approximation for transition energies between about 2.5 and 8 MeV; for instance, the three $E1$ curves are indistinguishable. Thus, a change in α can be simulated by a change in ω, and we can hold α fixed and vary ω only. This is convenient since $\mathcal{E}_l'(\omega)/\mathcal{E}_l'(2\pi)$ has a much simpler dependence on ω than on α. The efficiency ratio $\mathcal{E}_l'(\omega)/\mathcal{E}_l'(2\pi)$ was calculated for $\omega=90°$, 105°, and 120° for $\alpha=45.7°$ for transition energies from 1 to 8 MeV, for $E0$ and the first four orders of El and Ml tran-

sitions. For each value of ω, $C(\omega)$ was determined by a least-squares fit to the seven $E1$ transitions and then this value of $C(\omega)$ was used to obtain the $R_\omega(l)$ for other multipolarities. The $R_\omega(l)$, for $\omega=120°$ with $C(\omega)=3.49$, gave a good fit to the experimental results as shown in Fig. 14.

These are two reasons why the value of $\omega(=120°)$ determined from a comparison with the experimental R_ω is larger than the geometrical value of $\omega(=105°)$. First, the effect of the tilted sectors, i.e., 172° between the β_+ and β_- sectors, is to give an effective value of ω of 108°. Second, the rate of change of $R_\omega(l)$ with α is about five times the rate of change of $R_\omega(l)$ with ω. Thus, if α were one degree smaller (the measured value has an uncertainty of $\pm 1°$) the best fit would have occurred for $\omega \cong 115°$. Third, the effects of finite angular resolution on the efficiency with the baffle in place can be accurately simulated by decreasing α, and thus by increasing ω; and this effect is estimated to correspond to 1 or 2 degrees in α or $\simeq 5$ or 10° in ω for the full annulus opening. We note that the value of $C(\omega)$ obtained for $\omega=120°$ has little relation to the geometrically determined value since the most important effect on $C(\omega)$ of varying ω is due to the change in the solid angle subtended by the sector (with angle ω) at the annulus.

The degree to which the method described in this paper distinguishes between multipoles can be determined from an examination of Fig. 14. We see that for pure multipoles and transition energies greater than about 3 MeV there will usually be no difficulty in identifying $E0$, $E1$, or $E2$ transitions as long as the experimental errors for the 14 transitions of Fig. 14 are

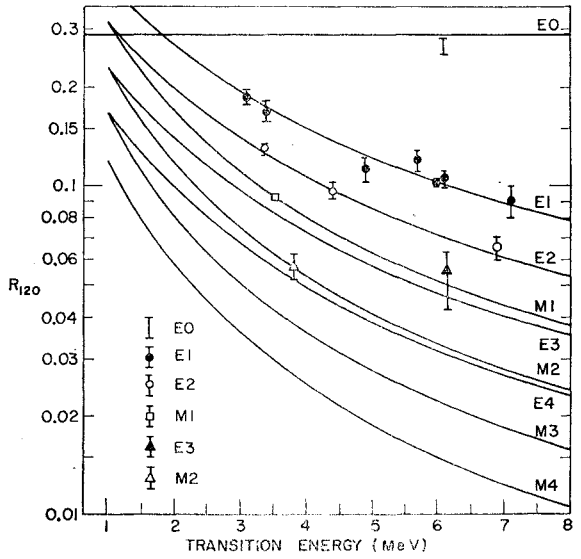

FIG. 14. Comparison for 14 known transitions, of the corrected experimental ratios R_{120} with the calculated values of $R_{120}(l)$. The calculated curves have been normalized to the experimental data by applying the least-squares method to the seven $E1$ transitions.

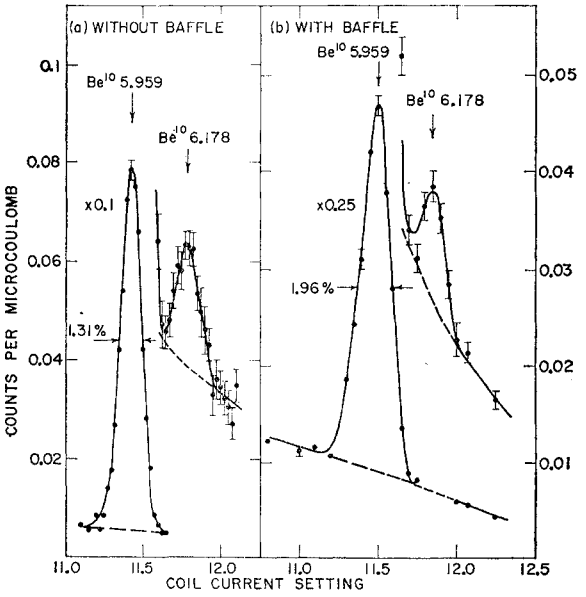

FIG. 15. The Be^{10} 5.959- and 6.178-MeV pair lines obtained (a) without the baffle and (b) with the baffle.

representative. For instance, at 6 MeV, the baffle-in to baffle-out ratios $R_{120}(l)$, are in proportions 4.25:1.46:1.0:0.73 for $E0$, $E1$, $E2$, and $M1$, respectively. Thus, a measurement of R_{120} to 10% or better could distinguish among these possibilities, as is clear from Fig. 14. The values of $R_{120}(l)$ for $M1$ and $E3$ are quite close together and the present method could not distinguish between these two multipolarities except in very favorable cases. The same is true for $M2$ and $E4$. However, the situation in which one of the two possibilities of $M1$ and $E3$ or of $M2$ and $E4$ could not be ruled out by other evidence would be rare indeed.

For the majority of the transitions listed in Table II the results of Fig. 14 confirm the multipolarities assigned from previous work. Some of the multipolarity assignments given in Table II are from indirect evidence or are not absolutely certain; thus, the present results can be said to confirm the multipolarity assignments of Table II. We also note that some of the transitions of Table II may have admixtures of higher multipolarities, however, the present results are consistent with the assumption that all 14 are pure multipoles.

Now that the theoretical ratios $R_\omega(l)$ have been calibrated using the effective value of 120° for ω we can use the results (the curves of Fig. 14) to assign multipolarities to other transitions. Experiments and results for some transitions in Be^{10}, B^{10}, C^{14}, and N^{14} are discussed in the next section.

V. SOME TRANSITIONS IN Be^{10}, B^{10}, C^{14}, AND N^{14}

A. Experimental Procedure and Results

In our investigations of the Be^9+d reactions, we studied the transitions Be^{10} 6.18 → 0, B^{10} 5.16 → 0.72,

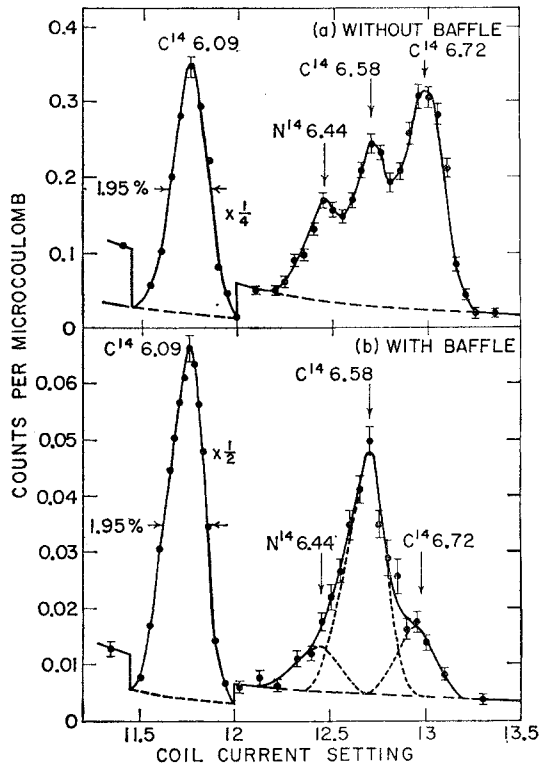

FIG. 16. Four ground-state transitions in C^{14} and N^{14} obtained (a) without the baffle and (b) with the baffle. The lines are identified by the nucleus to which they are assigned and the energies of the transitions are in MeV.

B^{10} $3.58 \rightarrow 0$, and B^{10} $3.58 \rightarrow 0.72$. These transitions were examined previously[13] with the pair spectrometer, but without the baffle system.

The B^{10} $5.16 \rightarrow 0.72$, $3.58 \rightarrow 0$ and $3.58 \rightarrow 0.72$ pair lines were measured using identical conditions and during the same runs as for the Be^{10} $3.37 \rightarrow 0$ transition listed in Table I. The conditions for the Be^{10} $6.18 \rightarrow 0$ transition were the same as for the Be^{10} $5.96 \rightarrow 0$ transition given in Table I. For the Be^{10} $6.18 \rightarrow 0$ transition the experimental results are illustrated in Fig. 15 which shows the Be^{10} $5.96 \rightarrow 0$ and $6.18 \rightarrow 0$ doublet taken with and without the baffle. From this figure it is found that the intensity of the $6.18 \rightarrow 0$ transition increases relative to that of the $5.96 \rightarrow 0$ transition by a factor of about 2.5 when the baffle is inserted. This indicates that the Be^{10} $6.18 \rightarrow 0$ transition is $E0$ and thus that the Be^{10} 6.18-MeV level is 0^+, an assignment which was suspected earlier.[13] The study of the Be^{10} $6.18 \rightarrow 0$ transition was a severe test of the method since this transition is quite weak at the highest bombarding energy available to us, and is separated by only 3% in energy[13] from the strong Be^{10} $5.96 \rightarrow 0$ transition.

Transitions in C^{14} and N^{14} were investigated using the $C^{13}+d$ reaction. The transitions studied were the $6.72 \rightarrow 0$ and $6.58 \rightarrow 0$ transitions in C^{14} and $7.03 \rightarrow 0$, $6.44 \rightarrow 0$, and $5.10 \rightarrow 0$ transitions in N^{14}. Previous pair-spectrometer work on these transitions (without the baffle system) has been reported.[20] All these transitions were studied using the conditions summarized for the N^{14} and C^{14} lines listed in Table I except for the N^{14} $7.03 \rightarrow 0$ transition which was investigated at a deuteron energy of 3.1 MeV.

Experimental results for three of the five transitions are illustrated in Fig. 16. This figure shows an unresolved triplet and the C^{14} $6.09 \rightarrow 0$ $E1$ transition. The changes that can occur in the relative intensities of pair lines when the baffle is inserted is illustrated quite clearly in this figure. The fact that the intensity of the C^{14} $6.58 \rightarrow 0$ transition increases relative to that of the $E1$ $6.09 \rightarrow 0$ transition by a factor of about 2.5 is consistent with the $E0$ assignment previously given for this transition,[20] while the decreased intensities of the $6.44 \rightarrow 0$ and $6.72 \rightarrow 0$ transitions show that they have multipolarities of order higher than $E1$. The transitions shown in Fig. 16 provided another severe test of the method. These data were collected in about 30 h with a resolution of 1.95%. Although the lines were not completely resolved, better resolution was not used because the time necessary to obtain sufficient statistics goes up rapidly with decreasing resolution and the C^{13} target showed signs of deterioration with bombardment. Reasonably accurate values of R_{120}' could be obtained from the data of Fig. 16 in spite of the fact that the lines are not resolved. This is so because the spectrometer line shape is independent of energy and is accurately known.

The measured values of R_{120}' for the transitions studied are given in Table III in which is also listed the available information on the A_ν coefficients for the gamma-ray transitions. The A_ν for the three transitions in B^{10} are taken from previous work.[13] The A_ν for the N^{14} $5.10 \rightarrow 0$ and C^{14} $6.72 \rightarrow 0$ transitions were obtained from three-crystal pair spectra of the gamma rays from bombardment of a C^{13} target of the same thickness as the one used in the present work.[26] Data were taken at seven angles between 0° and 90° to the beam at $E_d = 2.7$ MeV. The three-crystal pair spectra were similar to $C^{13}+d$ spectra taken previously at this laboratory[27] but had slightly better resolution.

The fourth and fifth columns of Table III list assumed multipolarities and the R_{120} obtained for these multipolarities from the R_{120}' (second column) and the A_ν coefficients (third column). In Fig. 17 the R_{120} values are compared with the theoretical curves of $R_{120}(l)$ which are taken from Fig. 14. The conclusions concerning the multipolarities of the nine transitions studied are given in the last column of Table III. The methods used to obtain the R_{120} and to arrive at these multipolarity assignments are discussed in detail in the next subsection.

---

[26] We would like to thank J. W. Olness and D. J. Bredin who assisted in the $C^{13}+d$ three-crystal pair-spectrometer work.

[27] E. K. Warburton and H. J. Rose, Phys. Rev. **109**, 1199 (1958).

TABLE III. Summary of the experimental results for some transitions in Be^{10}, B^{10}, C^{14}, and N^{14}.

Transition	R_{120}'	A_ν	Assumed multipolarity	R_{120}	Multipolarity (final result)
B^{10} 3.58 → 0.72	0.142±0.006	$A_2=A_4=+(0.014\pm0.04)$	$M1$	0.142±0.007	$M1$, $E2$
B^{10} 3.58 → 0	0.111±0.005	$A_2=+(0.03\pm0.05)$ $A_4=-(0.01\pm0.08)$	$M1$	0.111±0.006	$M1$, $E2$
B^{10} 5.16 → 0.72	0.088±0.006	$A_2=+(0.27\pm0.1)$ $A_4=0$	$M1$	0.079±0.006	$M1$, $E2$
N^{14} 5.10 → 0	0.120±0.007	$A_2=+(0.02\pm0.04)$ $A_4=+(0.04\pm0.05)$	$E1$	0.120±0.007	$E1$
Be^{10} 6.18 → 0	0.26 ±0.04	$A_\nu=0$	$E0$	0.26 ±0.04	$E0$
N^{14} 6.44 → 0	0.067±0.010	...	...	0.067±0.010	$E2$ or $M2$, $E3$
C^{14} 6.58 → 0	0.28 ±0.03	$A_\nu=0$	$E0$	0.28 ±0.03	$E0$
C^{14} 6.72 → 0	0.042±0.005	$A_2=+(0.51\pm0.04)$ $A_4=+(0.02\pm0.05)$	$M2$ or $E3$	0.035±0.005	$M2$ or $E3$
N^{14} 7.03 → 0	0.055±0.008	...	...	0.055±0.008	$M1$, $E2$ or $E1$, $M2$

B. Comparison with Theory

The Be^{10} 6.18 → 0 and C^{14} 6.58 → 0 Transitions

Since the ground states of Be^{10} and C^{14} have $J^\pi=0^+$, these transitions are $E0$ if the emitting states are also 0^+ in which case $A_\nu=0$ for $\nu>0$ and $R_{120}=R_{120}'$. As is clear from inspection of Fig. 17, both of these transitions have values for R_{120}' which are in agreement with $E0$ assignments. In order to make rigorous assignments of $E0$ to these transitions we must rule out the possibility that the emitting state is not 0^+ and aligned strongly such that R_{120}' is several times R_{120}. Consider first an assignment of 1^- or 1^+ to the Be^{10} 6.18- or C^{14} 6.58-MeV levels, then the transitions are $E1$ or $M1$. From Fig. 9 we find that for a 6-MeV transition $R_{120}(l)/R_{120}'(l)\geqslant 0.91$ for $E1$ and $\geqslant 0.83$ for $M1$. Since the $\Delta_2(\omega)$ are slowly varying functions of energy in the region of interest these limits hold for both the Be^{10} 6.18 → 0 and C^{14} 6.58 → 0 transitions. To obtain upper limits on $R_{120}(l)/R_{120}'(l)$ for quadrupole radiations we need the general expressions for the $A_\nu(22)$ for a 2 → 0 transition. These can be obtained from Eq. (14) and are

$$A_2(22)=-(5/7)[1-2P(0)-3P(1)],$$
$$A_4(22)=-(2/7)[1+5P(0)-10P(1)], \quad (21)$$

for a 2 → 0 quadrupole transition. In Eq. (21) the $P(m_i)$ are normalized so that $\sum_{m_i}P(m_i)=1$ and $P(2)$ has been eliminated using this normalization condition.

TABLE IV. Comparison of the minimum possible experimentally determined values of R_{120} with the theoretical $R_{120}(l)$ from Fig. 17 for various assumed multipolarities for the Be^{10} 6.18 → 0 transition. Experimentally $R_{120}'=0.26\pm0.04$.

Multipolarity	$[R_{120}(l)/R_{120}'(l)]_{\min}$	$[R_{120}(l)/R_{120}'(l)]_{\min}R_{120}'$	$R_{120}(l)$
$E0$	1.0	0.26±0.04	0.294
$E1$	0.91	0.24±0.03	0.100
$E2$	0.52	0.14±0.02	0.069
$M1$	0.83	0.22±0.03	0.050
$E3$	0.59	0.15±0.02	0.046
$M2$	0.43	0.11±0.02	0.033

By using Eqs. (18) and (21) and the $\Delta_\nu{}^{ll}(\omega)$ of Figs. 5–8, we can express $R_{120}(E2)/R_{120}'(E2)$ as a function of $P(0)$ and $P(1)$ and find the minimum value consistent with the allowable limits $0\leqslant P(0)\leqslant 1$, $0\leqslant P(1)\leqslant 0.5$, and $P(0)+2P(1)\leqslant 1$. The same procedure can also be followed for an $E3$ transition. The results for the Be^{10} 6.18 → 0 transition for $E0$, dipole, quadrupole, and $E3$ transitions are summarized in Table IV. From this table we see that only for an $E0$ assignment is agreement between theory and experiment for R_{120} possible. Since the C^{14} 6.58 → 0 transition has a measured R_{120}' slightly higher and with smaller uncertainties than for the Be^{10} 6.18 → 0 transition and since the $\Delta_\nu{}^{ll}(\omega)$ are not very sensitive to transition energy the same conclusions which can be drawn from Table IV hold for that transition also. The $\Delta_\nu{}^{ll}(\omega)$ for $M3$ or $l>3$ have not been calculated. Also, for the case of $E3$ radiation, it was assumed that $\nu\leqslant 4$ by virtue of one or more of the possible selection rules. Thus, a rigorous elimination

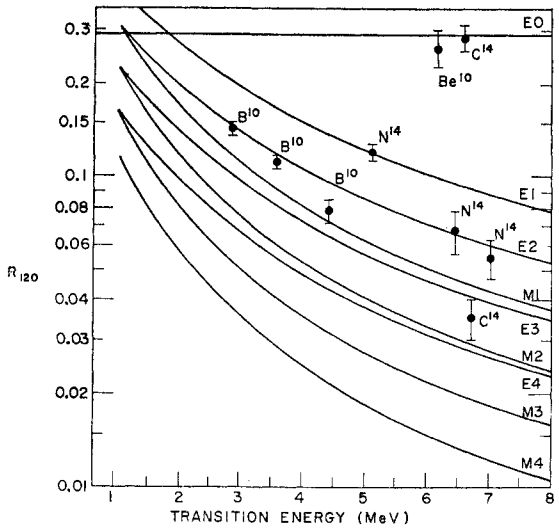

FIG. 17. Results of determinations of R_{120} for some transitions in Be^{10}, B^{10}, C^{14}, and N^{14}. The transitions are discussed in the text.

of multipolarities with $l>2$ was not made for these two transitions; however, it is clear, on the basis of the present results that the possibility that either transition is not $E0$ is sufficiently remote to be neglected. This follows from the facts: (1) a very strong and highly specialized alignment (or angular distribution of the competing gamma ray) is necessary in order that $R_{120}(l)/R_{120}'(l)$ be near its lower limit, (2) the value of $R_{120}(l)/R_{120}'(l)$ necessary to achieve agreement with experiment diminishes rapidly as l increases, and (3) on the basis of the results of Table IV it is doubtful that the minimum value of $R_{120}(l)/R_{120}'(l)$ will be low enough to achieve this agreement for $l>2$ since it does not occur for $l=1$ or 2. Also, for the Be^{10} $6.18\rightarrow 0$ transition we have the argument that in earlier work[13] it was found that the Be^{10} $6.18\rightarrow 3.37$ transition is less than 2.5 times as strong as the Be^{10} $6.18\rightarrow 0$ transition if the Be^{10} 6.18-MeV level is not 0^+. Since the Be^{10} 3.37-MeV level is 2^+ this limit rules strongly against $J>2$ for the Be^{10} 6.18-MeV level since the multipolarity of the Be^{10} $6.18\rightarrow 3.37$ transition would be two orders lower than that of the $6.18\rightarrow 0$ transition for $J>2$. And for the C^{14} $6.58\rightarrow 0$ level we have the fact that if the C^{14} 6.58-MeV level had $J>2$, the present results would demand that the cross section for its production in the $C^{13}+d$ reaction were comparable to that for the 6.72-MeV level (see Fig. 16) and that the angular distribution of the $6.58\rightarrow 0$ transition was strongly anisotropic. In this case the presence of the $6.58\rightarrow 0$ transition would have been readily apparent in at least one of the three-crystal pair spectra taken at seven angles to the beam. In actual fact, there was no evidence for this line at all.

In summary we conclude, as shown in Table III, that the Be^{10} 6.18- and C^{14} 6.58-MeV levels are both $J^\pi=0^+$. The theoretical implications of these assignments have been discussed previously.[13,20]

The C^{14} 6.72 → 0 Transition

$C^{13}(d,p)C^{14}$ stripping results have shown that the C^{14} 6.72-MeV level is 1^-, 2^-, or 3^- with a preference for the latter two.[28] By using Eq. (18), Figs. 5–8, and the A_ν given in Table III, we find $R_{120}(l)/R_{120}'(l)=0.84\pm0.04$ and 0.80 ± 0.07 for assignments to the C^{14} $6.72\rightarrow 0$ transition of $M2$ and $E3$, respectively. These corrections are close enough so that we can adopt a single value for R_{120}, namely, 0.035 ± 0.005. This value is shown in Fig. 17. It is apparent that the experimental error is too large to distinguish between $M2$ and $E3$. However, since the correction to R_{120}' for alignment is only a few percent for $E1$ (see Fig. 9), the present results definitely rule out the $J^\pi=1^-$ assignment as did previous work.[27,29]

[28] F. Ajzenberg-Selove and T. Lauritsen, Nucl. Phys. **11**, 1 (1959).

[29] A. A. Jaffe, De. S. Barros, P. D. Forsyth, J. Muto, I. J. Taylor and S. Ramavataram, Proc. Phys. Soc. (London) **76**, 914 (1960).

It is interesting to note that the angular distribution of the $C^{13}(d,p)C^{14}$ $(6.72\rightarrow 0)$ transition obtained from the three-crystal pair-spectrometer work is in excellent agreement with the predictions of plane-wave stripping for the preferred assignment[29] of 3^- to the C^{14} 6.72-MeV level. For a $3^-\rightarrow 0^+$ transition initiated by the $C^{13}(d,p)C^{14}$ reaction with $l_n=2$ the prediction is[22] (see Sec. IVA)

$$W(\theta)=1+0.86Q_2P_2(\theta)+0.143Q_4P_4(\theta). \qquad (22)$$

Based on the plane-wave stripping theory good approximations to Q_2 and Q_4 should be 0.64 and 0.18, respectively. These result in the predicted values $A_2=+0.55$ and $A_4=+0.025$, in excellent agreement with the experimental values given in Table III. For a 2^- assignment the predicted angular distribution has an additional uncertainty due to the unknown channel spin mixture and can be brought into agreement with experiment by choosing the right channel spin mixture. For the favored channel spin mixture (appropriate to the 6.72-MeV level being formed by adding a $d_{5/2}$ neutron to C^{13}) the prediction is $A_2=+0.32$, $A_4=0$—so that the gamma-ray angular distribution slightly favors the 3^- assignment.

The N^{14} 6.44 → 0 Transition

This transition was too weak for the gamma-ray angular distribution to be obtained from the three-crystal pair spectra. The uncorrected experimental value for R_{120}' is shown in Fig. 17. It has recently been shown that the N^{14} 6.44-MeV level is $J^\pi=3^+$ and that the 6.44-MeV transition to the 1^+ ground state of N^{14} is predominantly $E2$.[30] As may be seen in Fig. 17, the experimental determination of R_{120}' is consistent with an $E2$ assignment, but since the A_ν coefficients were not measured, an $M2$, $E3$ mixture, although unlikely, cannot be ruled out rigorously from our results alone.

The N^{14} 7.03 → Transition

As discussed previously[20] this transition can have a contribution from the ground-state decay of the C^{14} 7.01-MeV level, but it is unlikely that this contribution is very large and it is neglected in this discussion. The A_ν coefficients were not determined for the $7.03\rightarrow 0$ transition so the uncorrected R_{120}' is shown in Fig. 17. The N^{14} 7.03-MeV level has $J=2$, unknown parity. The measurement of R_{120}' indicates that the $7.03\rightarrow$ transition is not $E0$ or pure $E1$. It could be either a mixture of $M1$ and $E2$ or of $E1$ and $M2$.

The B^{10} 5.16 → 0.72 Transition

The alignment correction for this transition was made assuming it was $M1$. The resulting value of R_{120} is shown in Fig. 17. It is in agreement with the R_{120}

[30] H. Kuan, T. A. Belote, J. R. Risser, and T. W. Bonner, Bull. Am. Phys. Soc. **8**, 125 (1963); and private communication from H. Kuan.

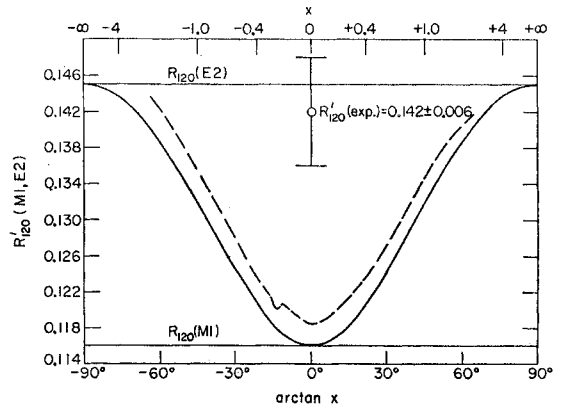

FIG. 18. The ratio of $R_{120}'(M1,E2)$ as a function of the M1, $E2$ mixing parameter x for the B^{10} $3.58 \rightarrow 0.72$ transition. The horizontal lines, R_{120} $(M1)$ and R_{120} $(E2)$ are the calculated ratios for nonalignment and pure $M1$ and $E2$ transitions, respectively. The solid curve is the nonaligned value, R_{120} $(M1,E2)$, and the dashed curve is the largest value of R_{120}' $(M1,E2)$ consistent with one standard deviation from the measured values of A_2 and A_4 (see text). The measured value of R_{120}' is also shown.

expected for an $M1$ transition but is not accurate enough to give useful information on the relative intensity of $E2$ radiation.

The B^{10} 0.72-MeV level is 1^+. The measurement of R_{120}' shows that the $5.16 \rightarrow 0.72$ transition cannot be $E1$ and since the speed of this transition is great enough to establish it as dipole,[13] the present result demands that the B^{10} 5.16-MeV level have even parity. There has been a great deal of confusion in the literature as to the spin-parity of the B^{10} 5.16-MeV level (it is now virtually certain that it is $J^\pi = 2^+$)[13] so that the present confirmation of the even parity assignment is of some value.

The B^{10} 3.58 → 0.72 Transition

If we assume this $2^+ \rightarrow 1^+$ transition is pure $M1$ the alignment correction is

$$R_{120}(M1)/R_{120}'(M1) = (1.0 \pm 0.03),$$

giving $R_{120} = 0.142 \pm 0.07$ (Table III). This value which is shown in Fig. 17 is clearly in poor agreement with a pure $M1$ assignment to the B^{10} $3.58 \rightarrow 0.72$ transition. An $M1$, $E2$ mixture must be invoked in order to achieve agreement between the measured R_{120}' and theory, so that the procedure we shall follow is to calculate the theoretical value of $R_{120}'(M,E)$ from Eq. (19) as a function of the $M1$, $E2$ mixing parameter x and to compare this to the measured value of R_{120}' to obtain information on x^2 (the intensity ratio of $E2$ to $M1$ radiation).

For a 2.86-MeV transition Eq. 19 becomes

$$R_{120}'(M1,E2) = \frac{0.116 + 0.175x^2 + N_{M1,E2}(120°)}{1 + 1.20x^2 + N_{M1,E2}(2\pi)}, \quad (23)$$

where $\mathcal{E}_{E2}'(2\pi)/\mathcal{E}_{M1}'(2\pi)$ is taken from Figs. 2 and 3 of Wilkinson, *et al.*[12] and $R_{120}(M1)$ and $R_{120}(E2)$ are taken from Fig. 14 or Fig. 17. For this transition we found (see Table III) $A_2 = A_4 = +(0.014 \pm 0.04)$ which is consistent with the initial state being nonaligned. If it is nonaligned, then the $N_{M1,E2}(\omega)$ of Eq. (21) are zero. In the case the variation of $R_{120}'(M1,E2)$ is given by the solid curve of Fig. 18 which shows $R_{120}'(M1,E2)$ plotted against x for $-\infty \leqslant x \leqslant +\infty$. The experimental value of R_{120}' is also shown in Fig. 18 and we find that for nonalignment of the B^{10} 3.58-MeV state the measured value of R_{120}' which is consistent with $x^2 = \infty$, gives $|x| > 1.4$, 0.9 and 0.56 for 1, 2, and 3 standard deviations below the measured value, respectively. Since the measured values of A_2 and A_4 do not rule out some alignment effects, we need to calculate the possible deviations of $R_{120}'(M1,E2)$ from the solid curve of Fig. 18 due to the largest degree of alignment consistent with $A_2 = A_4 = +(0.014 \pm 0.04)$.

For a $2^+ \rightarrow 1^+$ $M1$, $E2$ transition, Eqs. (12) and (14) give

$$\begin{aligned} A_2 &= F_2(2)(0.5 + 2.236x - 0.3566x^2)/(1+x^2), \\ A_4 &= F_4(2)0.1904x^2/(1+x^2), \end{aligned} \quad (24)$$

where

$$\begin{aligned} F_2(2) &= 1 - 2P(0) - 3P(1), \\ F_4(2) &= 1 + 5P(0) - 10P(1). \end{aligned} \quad (25)$$

Using Eq. (24) and obtaining the $\Delta_\nu^{ll'}(\omega)$ from Figs. 5–8 we find, from Eq. (20),

$$\begin{aligned} N_{M1,E2}(2\pi) &= [0.23 + 0.76x - 0.235x^2]F_2(2) \\ &\quad - 0.069x^2F_4(2), \quad (26) \\ N_{M1,E2}(120°) &= 0.116[0.44 + 1.63x - 0.61x^2]F_2(2) \\ &\quad - 0.004x^2F_4(2). \end{aligned}$$

Limits on $F_2(2)$ and $F_4(2)$ are given by the measured values of A_2 and A_4 which give

$$\begin{aligned} F_2(2) &= \frac{+(0.014 \pm 0.04)(1+x^2)}{0.5 + 2.236x - 0.3566x^2}, \\ F_4(2) &= \frac{+(0.014 \pm 0.04)(1+x^2)}{0.1904x^2}, \end{aligned} \quad (27)$$

subject to the conditions implied by Eq. (25), i.e., $-1 \leqslant F_2(2) \leqslant +1$, $-4 \leqslant F_4(2) \leqslant +6$ with the values of $F_2(2)$ and $F_4(2)$ interdependent. By using Eqs. (26) and (27) to obtain the $N_{M1,E2}(\omega)$, the value of $R_{120}'(M1,E2)$ corresponding to one standard deviation (for A_2 and A_4) above the nonaligned value is obtained and is shown by the dashed curve in Fig. 18 which is plotted for $|x| < 2$. The cusp-like behavior in this curve at $x = -0.26$ is due to the fact that both quadratics in x in Eq. (26) have zeros near this value of x. From the dashed curve of Fig. 18 we find $|x| > 1.0$, 0.70, 0.42 ($x^2 > 1.0, 0.49, 0.17$) for 1, 2, and 3 standard deviations

below the measured value of R_{120}'. We adopt 0.7 as the lower limit for $|x|$.

Shafroth and Hanna[31] studied the angular correlation of the B^{10} $3.58 \rightarrow 0.72 \rightarrow 0$ cascade. As discussed previously,[13] their results demand $0.12 \leqslant x \leqslant 0.45$ or $|x| > 6$ for the B^{10} $3.58 \rightarrow 0.72$ transition. The present results are inconsistent with the range $0.12 \leqslant x \leqslant 0.45$ but in agreement with the range $|x| > 6$.

The radiative widths of the B^{10} 3.58-MeV level decay have been calculated on the independent-particle model (IPM) by Kurath[32] and Soper.[33] For the $3.58 \rightarrow 0.72$ transition Kurath found $x^2 = 0.1$–0.2 for the favored range of 3–5 for the intermediate coupling parameter a/K, while Soper, who took collective enhancement into account in the weak-coupling approximation, found $x^2 = 0.15$–0.35 in the same range. Thus, the present result, $x^2 > 0.5$ is in disagreement with the IPM but not severely so. However, the IPM is in severe disagreement with the limit $|x| > 6$ demanded by the combined results of Shafroth and Hanna[31] and the present work. In view of this disagreement a remeasurement of the B^{10} $3.58 \rightarrow 0.72 \rightarrow 0$ angular correlation would appear to be worthwhile.

The B^{10} 3.58 → 0 Transition

The analysis of the results for this transition is identical with that for the B^{10} $3.58 \rightarrow 0.72$ transition. For an assumption of pure $M1$ radiation the alignment correction is $R_{120}(M1)/R_{120}'(M1) = (1.0 \pm 0.03)$ giving $R_{120} = 0.111 \pm 0.006$ (Table III). As is shown in Fig. 17 this value is in disagreement with a pure $M1$ assignment. By assuming nonalignment of the B^{10} 3.58-MeV level we find that the measured value of (0.111 ± 0.005) for R_{120}' gives $|x| = 2^{+\infty}_{-1}$ with $|x| > 1.1$, 0.78, and 0.5 for 1, 2, and 3 standard deviations below the measured value. If the effects of nonalignment are taken into account in the same manner as for the B^{10} $3.58 \rightarrow 0.72$ transition, we find $|x| > 0.7$, 0.45, and 0.15 ($x^2 > 0.49$, 0.2, 0.02) for 1, 2, and 3 standard deviations below the measured value of R_{120}'. We adopt the limit $|x| > 0.45$ ($x^2 > 0.2$).[33a]

The IPM calculations of Soper[33] give $x^2 = 0.21$ for $a/K = 3$–5 which is not in severe disagreement with our results.

The N^{14} 5.10 → 0 Transition

The N^{14} 5.10-MeV level has $J = 2$, $T = 0$ and unknown parity.[28] If we assume that this $2 \rightarrow 1^+$ transition is $E1$ the alignment correction is negligible so that $R_{120}' = R_{120}$. The measured value of R_{120}' which is shown in Fig. 17, is in excellent agreement with the predicted value for an $E1$ transition. The possibility that this transition is an $M1$, $E2$ mixture with a strong alignment-interference correction to R_{120}' is easily ruled out from the measured A_ν coefficients (Table III) and an analysis identical to that described for the B^{10} $3.58 \rightarrow 0.72$ transition. Thus, the N^{14} $5.10 \rightarrow 0$ transition is predominately $E1$ and the N^{14} 5.10-MeV level has odd parity.

It has recently been shown that the N^{14} 5.10- and 5.83MeV levels have the same parity.[34,35] Thus, the parity of the N^{14} 5.83-MeV level is odd. The odd-parity assignments for these two levels are in agreement with the prediction of Warburton and Pinkston.[36]

Because of the inhibition of $\Delta T = 0$, $E1$ and $M2$ transitions in light self-conjugate nuclei,[37] and the possible collective enhancement of $E3$ transitions for the same conditions, the N^{14} $5.10 \rightarrow 0$ transition could very well contain significant contributions of $E1$, $M2$, and $E3$ radiation. Because the alignment correction for $E1$ transitions is so small (see Figs. 5 and 7), upper limits to the admixtures of $M2$ and $E3$ radiation can be estimated from the measured value of R_{120}' using the nonaligned formula for $R_{120}'(E1,M2)$ and $R_{120}'(E1,E3)$. Using Eq. (18), we find that the limits corresponding to one standard deviation below the measured value of R_{120}', 0.120 ± 0.007, are $x^2(E1,M2) < 0.10$ and $x^2(E1,E3) < 0.13$ assuming negligible $E3$ and $M2$ radiation, respectively. We double these limits to allow for interference effects and adopt $x^2(E1,M2) < 0.2$, $x^2(E1,E3) < 0.25$.

The N^{14} $5.10 \rightarrow 0$ transition was studied previously by the $C^{13}(p,\gamma)N^{14}$ reaction.[38] Assuming an $E1, M2$ mixture it was found that $x^2(E1,M2)$ was in the range $0.1 \leqslant |x| \leqslant 0.2$ or $4 \leqslant x \leqslant 6$. Our result of 0.2 as the upper limit on x^2 clearly rules out the second alternative and is consistent with the first.

VI. CONCLUSIONS

A critique of the method of measuring multipolarities which we have developed can be based largely on the results shown in Figs. 14 and 17. The ratios for the 14 transitions in Fig. 14 all have values of R_{120} in agreement with theory except for the O^{16} 6.06-MeV $E0$ transition. For this line we have recently obtained further evidence that the experimental R_{120} is smaller than predicted. The reason for this discrepancy is being investigated.

Although the transitions in Fig. 14 were all treated as calibration lines of known multipolarity several of these have not been established previously and the present

[31] S. M. Shafroth and S. S. Hanna, Phys. Rev. **104**, 399 (1954).
[32] D. Kurath, Phys. Rev. **106**, 975 (1957).
[33] J. M. Soper (private communication). Part of these results have been given in Ref. 13.
[33a] *Note added in proof.* The gamma radiation angular distribution coefficient A_2 for a $J = 2 \rightarrow J = 3$ transition was given incorrectly in Eq. (22) of Ref. 13. It should be

$$A_2 = F_2(2)(0.143 - 1.57x + 0.408x^2)/(1 + x^2).$$

[34] H. J. Rose, F. Uihlein, F. Reiss, and W. Trost, Nucl. Phys. **36**, 583 (1962).
[35] J. A. Becker, Phys. Rev. **131**, 322 (1963).
[36] E. K. Warburton and W. T. Pinkston, Phys. Rev. **118**, 733 (1960).
[37] E. K. Warburton, Phys. Rev. Letters **1**, 68 (1958).
[38] E. K. Warburton, H. J. Rose, and E. N. Hatch, Phys. Rev. **114**, 214 (1959).

results can be used to make these assignments definite. For example, from our measurements the Be^{10} 5.96-MeV transition to the Be^{10} 0^+ ground state is definitely not $M2$, and since the Be^{10} 5.96-MeV level is known from $Be^9(d,p)Be^{10}$ stripping results[18] to have $J^\pi=1^-$, or 2^-, the present results show that the Be^{10} 5.96-MeV level is 1^-.

Another example is the N^{14} 5.69-MeV level which has a spin of one.[18] The result shown in Fig. 14 for the 3.38-MeV transition from this level to the N^{14} 0^+ 2.31-MeV level definitely rules out an $M1$ assignment to the N^{14} $5.69 \rightarrow 2.31$ transition, leaving 1^- as the only possibility for the 5.69-MeV level.

This result for the N^{14} 5.69-MeV level demonstrates the advantages of the present technique over previous methods[1-3] of obtaining multipolarities from studies of the angular correlation of the internal pairs. Gorodetzky, *et al.*[3] measured the angular correlation of the N^{14} $5.69 \rightarrow 0$ transition using plastic scintillators to detect the $\beta_+ \beta_-$ pair and the $C^{13}(d,n)N^{14}$ reaction to populate the 5.69-MeV level. They were not able to resolve the 5.69-, 5.83-, and 6.09-MeV transitions which are produced from $C^{13}+d$,[20] so that their results were not conclusive and, in fact, agreed better with $M1$ for the N^{14} $5.69 \rightarrow 0$ transition than with the $E1$ assignment that our measurement requires.

The results shown in Fig. 17 and discussed in Sec. V illustrate quite clearly that the information obtainable from a measurement of the angular distribution of the competing gamma-ray transition is generally a necessary supplement to the spectrometer ratio measurement in order to make a clear-cut multipolarity assignment. In general, it is only for $E0$ transitions of $\gtrsim 3$ MeV or for proving that a transition is *not* $E1$ that the spectrometer measurement alone can give a definite answer without supporting information. However, exceptions to this rule will occasionally arise.

Our technique has a practical limit in momentum resolution of about 1%. Although we have not made measurements of spectra in which the various pair lines without the baffle have differed in intensity by a factor of more than 40, it should be possible to study favorable cases when the weakest line is $\lesssim 1\%$ of the strongest line. In the absence of beta-ray activities, whether or not ratio measurements can be made on a very weak line depends on the absolute yield or on the background of real coincidences due to the scattering of pairs associated with strong lines at higher energies. Except for the 6.06-MeV $E0$ line in O^{16} our highest yield was obtained for the 3.37-MeV transition in Be^{10} where the peak counting rate without the baffle was ~ 1000 per min. It should be possible to measure ratios for lines such that the yield without the baffle is only a few counts per min if the background is low enough. If high-energy and intense beta-ray activities are produced by the reaction used—such as is the case for the $B^{11}(d,p)B^{12}$ reaction—it may be difficult to detect any lines at all.

A question of interest is to what region of the periodic table is the method applicable? This question has two aspects. First, the plane-wave Born approximation which we rely on will be inadequate to describe the internal pair formation in the heaviest nuclei. Its range of validity, which has been discussed previously,[12] depends critically on the energy of the transition. We expect that the Born approximation would be adequate for the present purpose for $Z<30$ if $E_\gamma>3$ MeV. The second aspect of this question is that the sensitivity to multipolarity of the method may well persist even to the heaviest nuclei. If so, then the ratios $R_\omega(l)$ could be obtained empirically or by a theoretical calculation which would include the effect of the Coulomb field.

As mentioned previously we have now constructed a new spiral baffle system which has very nearly the same arrangement of baffle blades as described in this paper but which can be moved in and out of place without breaking the vacuum. Another feature of the new system is that the baffle can be rotated by 90°. The result (refer to Fig. 11) is that positron-electron pairs for which $0° \leq \theta \lesssim 50°$ are detected selectively for this orientation of the baffle. Although the calculations of efficiency have not yet been carried out for this case it is clear that the ratio $Y_{\text{with baffle}}/Y_{\text{rotated baffle}}$ will be more sensitive to multipolarity than the ratio $Y_{\text{with baffle}}/Y_{\text{without baffle}}$; but it is not clear whether the gain in sensitivity will be enough to compensate for the loss of intensity between $Y_{\text{without baffle}}$ and $Y_{\text{rotated baffle}}$. It is also possible that a measurement of $Y_{\text{rotated baffle}}$ will provide useful information for estimating alignment effects on the R_ω'. The new baffle arrangement will be described in a forthcoming paper.

In this connection we may mention a suggestion made to us by Wilkinson. His proposal is to construct the "ideal" baffle system having 90° acceptance sectors and to make the detector in the form of four 90° quadrant-shaped crystals, all shielded from each other and connected to four photomultiplier tubes by means of light pipes. Referring to Fig. 11 we designate these four crystals as $1U$ (upper), $1L$ (lower), $2U$, and $2L$. For the system described in this paper we detect pairs for $50° \lesssim \theta \lesssim 90°$ by measuring the sum of $1L$, $2L$ and $1U$, $2U$ coincidences. Those pairs having $0° \leq \theta \lesssim 50°$ are not counted in the present arrangement (without rotating the baffle system) since they arrive in positions $1L$, $1U$ and $2L$, $2U$, i.e., they enter the same crystal. By having the four detectors and leaving the baffle system in the fixed position shown in Fig. 11 it would then be possible to measure the $50° \lesssim \theta \lesssim 90°$ pairs and the $0° \leq \theta \lesssim 50°$ pairs at the same time by making suitable connections to a multiple-channel coincidence circuit. Random coincidences could also be measured as the rates $1L$, $2U$ and $2L$, $1U$. In principle the ratio of counting rates

$$(1L,\ 2L+1U,\ 2U)-(1L,\ 2U+1U,\ 2L) \qquad \text{for} \quad 50° \lesssim \theta \lesssim 90°$$

and

$$(1L, 1U+2L, 2U)-(1L, 2U+1U, 2L) \quad \text{for} \quad 0°\leq\theta\lesssim 50°$$

should correspond to calculated reduction ratios much like the curves illustrated in Figs. 14 and 17. A small computer could be programed to continuously compare this ratio and its uncertainty to the predicted ratios for the energy of the pair line under study. This comparison could be made on a meter which could read directly the multipolarity of the transition, although the scheme would be practical only if the background were low enough. In this mode of operation the device could be truly designated as a "Multipole Meter."

ACKNOWLEDGMENTS

We would like to thank I. Cole, E. Windschauer, and R. Hirko who assisted in the calculations of the spectrometer efficiency and Professor D. H. Wilkinson for helpful discussions.